Artesunate protects against a mouse model of cerulein and lipopolysaccharide-induced acute pancreatitis by inhibiting TLR4-dependent autophagy

DAN LIU[1*], CHAO LIU[2*], FEI DENG[1*], FUMIN OUYANG[1], RONGXIN QIN[2], ZHAOXIA ZHAI[1], YAN WANG[1], YU ZHANG[1], MENGLING LIAO[1], XICHUN PAN[2], YASI HUANG[1], YANYAN CEN[2], XIAOLI LI[3,4] and HONG ZHOU[1]

[1]Key Laboratory of Basic Pharmacology of Ministry of Education and Joint International Research Laboratory of Ethnomedicine of Ministry of Education, Zunyi Medical University, Zunyi, Guizhou 563000, P.R. China; [2]Department of Pharmaceutical Chemistry, College of Pharmacy, Army Medical University (The Third Military Medical University), Chongqing 400016, P.R. China; [3]Department of Pharmacology, College of Pharmacy, Chongqing Medical University, Chongqing 400016, P.R. China; [4]Key Laboratory for Biochemistry and Molecular Pharmacology of Chongqing, Chongqing 400016, P.R. China

Received June 25, 2024; Accepted October 9, 2024

DOI: 10.3892/ijmm.2024.5466

Abstract. Severe acute pancreatitis (SAP) is a severe clinical condition associated with high rates of morbidity and mortality. Multiple organ dysfunction syndrome that follows systemic inflammatory response syndrome is the leading cause of SAP-related death. Since the inflammatory mechanism of SAP remains unclear, there is currently a lack of effective drugs available for its treatment. Therefore, it is important to study effective therapeutic drugs and their molecular mechanisms based on studying the inflammatory mechanism of SAP. In the present study, *in vivo*, a mouse model of AP induced by cerulein (CR) combined with lipopolysaccharide (LPS) was established to clarify the therapeutic effect of artesunate (AS) in AP mice by observing the gross morphological changes of the pancreas and surrounding tissues, calculating the pancreatic coefficient, and observing the histopathology of the pancreas. The serum amylase activity in AP mice was detected by iodine colorimetry and the superoxide dismutase activity in the pancreas was detected by WST-1 assay. The levels of proinflammatory cytokines in the serum, the supernatant of pancreatic tissue homogenates and the peritoneal lavage fluid were detected by ELISA assay. The total number of peritoneal macrophages was assessed using the cellular automatic counter, and the expression of proteins related to autophagy, and the TLR4 pathway was detected by immunohistochemistry and western blotting. *In vitro*, the effect of trypsin (TP) combined with LPS was observed by detecting the release of proinflammatory cytokine levels from macrophages by ELISA assay, and detecting the expression of proteins related to autophagy and the TLR4 pathway by immunofluorescence and western blotting. The present study revealed that AS reduced pancreatic histopathological damage, decreased pancreatic TP and serum amylase activities, increased superoxide dismutase activity, and inhibited pro-inflammatory cytokine levels in a mouse model of AP induced by cerulein combined with lipopolysaccharide. *In vitro*, TP combined with LPS was found to synergistically induce pro-inflammatory cytokine release from mouse macrophages and RAW264.7 cells, while AS could inhibit cytokine release. Furthermore, CR combined with LPS synergistically increased amylase activity in acinar cells, whereas AS decreased amylase activity. Autophagy serves an important role in the release of pro-inflammatory cytokines. In the present study, it was revealed that the autophagy inhibitor LY294002 suppressed the release of pro-inflammatory cytokines from macrophages treated with TP combined with LPS, and pro-inflammatory cytokine release was not further reduced by AS combined with LY294002. Furthermore, AS not only inhibited the expression of important molecules in the Toll-like receptor 4 (TLR4) signaling pathway, but also inhibited autophagy proteins and reduced the number of autolysosomes in mice with AP and in macrophages. In conclusion, these results suggested that AS may protect against AP in mice via inhibition of TLR4-dependent autophagy; therefore, AS may be considered a potential therapeutic agent against SAP.

Correspondence to: Professor Hong Zhou, Key Laboratory of Basic Pharmacology of Ministry of Education and Joint International Research Laboratory of Ethnomedicine of Ministry of Education, Zunyi Medical University, 1 Campus Road, Zunyi, Guizhou 563000, P.R. China
E-mail: zhouh64@163.com

Professor Xiaoli Li, Key Laboratory for Biochemistry and Molecular Pharmacology of Chongqing, 1 Medical College Road, Yuzhong, Chongqing 400016, P.R. China
E-mail: plum181181@126.com

*Contributed equally

Key words: acute pancreatitis, artesunate, lipopolysaccharide, cerulein, trypsin, autophagy

Introduction

Severe acute pancreatitis (SAP) is one of the most common and serious gastrointestinal inflammatory diseases, which is associated with high rates of morbidity and mortality. Notably, it has been reported that 20-30% of patients who develop SAP have a mortality rate as high as 20-40% globally (1,2).

The basis of AP is inflammation, in which pancreatic enzymes are activated and then cause inflammation of the pancreatic tissue, which locally manifests as pancreatic digestion, edema, bleeding and pancreatic necrosis. The injured pancreatic tissue releases a large amount of pro-inflammatory cytokines, including tumor necrosis factor α (TNF-α), interleukin (IL)-6 and IL-1β, triggering a cascade of inflammatory mediators, which develops rapidly from local inflammation into systemic inflammatory response syndrome (SIRS) (3). Inflammation is present throughout the pathophysiological course of AP; therefore, if SIRS is not controlled, sepsis, septic shock and multiple organ dysfunction syndrome (MODS), resulting from the presence of infectious factors (such as surgical infection), can occur (4,5).

Autophagy is an evolutionarily conserved self-protection mechanism that is closely related to the occurrence and development of inflammation. Under normal conditions, autophagy is maintained at a low level; however, starvation, stress, infection, immune disorders and other conditions can induce increased autophagy (6,7). Previous studies have shown that autophagy is involved in the inflammatory process of SAP (8,9), and the inhibition of key molecules in the process of autophagy can reduce the degree of inflammation in model animals with SAP (10).

Although the activation of trypsin (TP) in pancreatic tissue is considered a key cause of pancreatic tissue inflammation, experimental results have suggested that the activation of TP alone is insufficient, and lipopolysaccharide (LPS) from the gut may be involved in the development of pancreatitis (11-13). However, whether there is a synergistic effect between TP and LPS remains unclear.

Artesunate (AS) is a World Health Organization-approved first-line drug for the treatment of severe malaria in adults and children (14). In addition to its anti-malarial effects, in recent years, it has been shown that AS can exert notable anti-inflammatory and antitumor effects (15). In our previous study, AS was revealed to inhibit the Toll-like receptor 4 (TLR4)/nuclear factor-κB (NF-κB) signaling pathway, which could decrease digestive enzyme activity and pro-inflammatory cytokine expression, thereby improving survival in rats with SAP (16). However, the detailed molecular mechanism of AS in AP is not yet clear.

In the present study, the effects of AS on an animal model of AP induced by cerulein (CR) and LPS were investigated. Subsequently, the synergistic effects of TP and LPS on mouse macrophages, and CR combined with LPS on acinar cells were investigated, as well as the synergistic effects and molecular mechanisms of TP and LPS on mouse macrophages.

Materials and methods

Reagents. AS for injection was purchased from Guilin Pharmaceutical Co., Ltd. For the *in vivo* experiments, AS was dissolved in dimethyl sulfoxide (100%; 0.02 ml/10 g administration volume, determined to have no negative effect in preliminary experiments); for the *in vitro* experiments, AS was dissolved in 1 ml 5% sodium bicarbonate and then diluted in 0.9% sterile normal saline (NS).

LPS (from *Escherichia coli* O55:B5) was purchased from MilliporeSigma. CR was purchased from MedChemExpress (cat. no. HY-A0190). LY294002 were purchased from MedChemExpress (cat. no. HY-10108). TP was purchased from Nanjing Jiancheng Bioengineering Institute (cat. no. I015-1-1). The primary antibodies used for western blotting (WB) and immunofluorescence staining were: Anti-Beclin-1 (cat. no. 3738), anti-TNF receptor associated factor 6 (TRAF6; cat. no. 8028), anti-microtubule associated protein 1 light chain 3 (LC3; cat. no. 2775), anti-myeloid differentiation primary response 88 (MyD88; cat. no. 4283), anti-TLR4 (cat. no. 38519), anti-ATG16L1 (cat. no. 8089), anti-β-actin (cat. no. 4967) and anti-GAPDH (cat. no. 2118) (all from Cell Signaling Technology, Inc.). The secondary antibodies were horseradish peroxidase (HRP)-conjugated goat anti-rabbit (cat. no. SA00001-2) or anti-mouse (cat. no. SA00001-1) (both Proteintech Group, Inc.). The primary antibodies used for immunohistochemistry were: Anti-Beclin-1 (cat. no. A7353; ABclonal Biotech Co., Ltd.), anti-LC3 (cat. no. 2775; Cell Signaling Technology, Inc.) and anti-TLR4 (cat. no. ab22048; Abcam).

The enzyme-linked immunosorbent assay (ELISA) kits used to detect cytokines, including TNF-α (cat. no. BMS607-3TEN) and IL-6 (cat. no. KMC0061), were purchased from Thermo Fisher Scientific, Inc. The amylase (cat. no. C016-1-1), TP (cat. no. A080-2-2) and superoxide dismutase (SOD; cat. no. A001-3-2) assay kits were purchased from Nanjing Jiancheng Bioengineering Institute. The total protein extraction kit (cat. no. BB-3101) was purchased from BestBio Ltd. The 2-step plus Poly-HRP Anti Mouse/Rabbit IgG Detection System (with DAB solution) (cat. no. E-IR-R-217) was purchased from Elabscience Biotechnology Co., Ltd. Anti-rabbit Alexa Fluor 555 immunofluorescent staining kit (cat. no. P0179) was purchased from Beyotime Institute of Biotechnology. Autophagic double-labeled adenovirus HBAD-monomeric red fluorescent protein (mRFP)-green fluorescent protein (GFP)-LC3 (cat. no. HB-AP210 001) was purchased from Hanheng Biotechnology (Shanghai) Co., Ltd.

Animals. Kunming (KM) mice (age, 3-4 weeks; weight, 18-22 g) were obtained from Hunan SJA Laboratory Animal Co., Ltd. All mice were housed in a pathogen-free facility (temperature, 20-25˚C; humidity, 50-65%) at Zunyi Medical University (Zunyi, China) under a 12-h artificial light-dark cycle, and with *ad libitum* access to food and purified water. All protocols and experimental procedures involving live animals were approved by the Animal Care Welfare Committee of Zunyi Medical University [approval no. ZMU (2020) 2-296]. All of the experiments were conducted in compliance with the National and Institutional Guidelines for the Care and Use of Experimental Animals (17).

Cell lines, cell culture and mouse peritoneal macrophage (PM) purification. The mouse macrophage cell line RAW264.7 and the rat pancreatic exocrine cell line AR42J were obtained from

American Type Culture Collection. RAW264.7 cells were cultured in Dulbecco's modified Eagle's medium (DMEM; cat. no. 11965092; Gibco; Thermo Fisher Scientific, Inc.) supplemented with 10% (v/v) fetal bovine serum (FBS; Biological Industries; Sartorius AG) at 37˚C in 5% CO_2. AR42J cells were cultured in Ham's F-12K (Kaighn's) medium (F12K; cat. no. 21127022; Gibco; Thermo Fisher Scientific, Inc.) containing 10% FBS at 37˚C in 5% CO_2.

Murine PMs from normal male KM mice were isolated and cultured according to previously published methods (18,19). After each mouse was intraperitoneally injected with 10 ml NS, PMs were collected by aspiration, suspended in DMEM, added to a cell culture dish and incubated for 3 h at 37˚C in a humidified incubator containing 5% CO_2. Thereafter, the cells were washed with phosphate-buffered saline (PBS) to remove floating cells. Adherent cells were considered to be PMs with ~90% purity. All reagents and appliances used in the experiments were endotoxin-free.

Establishment of an animal model of AP and treatment. The mouse model of AP was established by the intraperitoneal injection of CR (100 μg/kg) once every hour for 6 h, followed immediately by the intraperitoneal injection of LPS (10 mg/kg) (20). Briefly, 28 KM mice were divided into four groups (n=6/group): i) The NS group was intraperitoneally injected with NS (0.1 mg/10 g); ii) the AP group received CR (100 μg/kg) intraperitoneally once an hour for 6 h, and the mouse model of AP was successfully established by intraperitoneal injection of LPS (10 mg/kg) immediately after the last CR injection; and the iii) AS5 + AP and iv) AS15 + AP groups, in which the mice were intraperitoneally injected with 5 or 15 mg/kg AS, respectively, immediately after the last injection of LPS.

The whole experiment lasted 24 h. During the experimental period, the health status of mice was observed every 2 h and the mortality rate of mice was 0%. The mice were euthanized through cervical dislocation at 2, 8 (28 mice each time) and 18 h (only 4 mice in the NS group with AP + AS15 and 5 mice in the AP group with AP + AS5) after model establishment to minimize the time required for loss of consciousness. In addition, predetermined humane endpoints were set, which if reached meant the animal experiments could not continue (21). The experiment was terminated when the mice appeared weak, and lost the ability to eat and drink on their own. Death was verified by the loss of heartbeat. No mice reached the humane endpoints.

Collection of serum, pancreatic tissue and peritoneal lavage fluid. A total of 2, 8 and 18 h after establishment of the AP model, serum was collected by removing the eyeballs from the sacrificed mice at the 2-h time point and leaving them for 2 h at room temperature. After centrifugation of the blood from the eye socket after eyeball removal was performed at 4˚C and 1,008 x g for 10 min, the supernatant was collected to detect pro-inflammatory cytokine levels and amylase activity.

In addition, mice were sacrificed by cervical dislocation at the 2-, 8- and 18-h time points. Mice were injected intraperitoneally with 5 ml PBS and rubbed gently for 2 min at the 2 h time point. The peritoneal lavage fluid was then aspirated using a pipette, centrifuged at 178 x g for 3 min at room temperature, and the pellet and supernatant were separated to detect the number of PMs and pro-inflammatory cytokine levels, respectively.

The pancreas was excised by laparotomy, observed visually to detect the presence or absence of edema, hyperemia and necrosis, and then images of the pancreatic tissue were captured at the 2-h time point. Detection of the pancreatic coefficients at the 8-h time point, and the pancreatic coefficient was calculated as follows: Wet gland weight (mg)/mouse weight (g). Subsquently, one-third of the pancreatic tissue (pancreatic tail) of each mouse was cut off for homogenization (45 Hz, 50 sec, three times) at the 2-h time point and the 18-h time point. Since the volumes and masses of the aforementioned pancreatic tissues from each mouse were different, different volumes of saline were added for homogenization according to the mass, in order to obtain the same mass concentration of the pancreatic tissue homogenate. Finally, the homogenates were centrifuged at 4˚C and 1,008 x g for 10 min, and the supernatant was obtained to detect pro-inflammatory cytokine levels (2-h time point), TP activity (18-h time point) and SOD activity (2-h time point).

The specific activity of an enzyme is internationally expressed as U/mg protein, which indicates the number of units of enzyme activity per unit weight (mg) of protein. Therefore, U/mg protein was used to express TP and SOD activities, according to the instructions of the kit manufacturer. Amylase activity, on the other hand, since there is no protein involved, was expressed in U/dl according to the kit manufacturer's instructions. The international unit of pro-inflammatory cytokines was formulated by the International Organization for Standardization (22) and is expressed in the form of international unit (IU). Different inflammatory factors have different IUs, for example, the IU of IL-1β is pg/ml (not used here), the IU of TNF-α is pg/ml or pg/10^6 cells and the IU of IL-6 is pg/ml or pg/10^6 cells. Therefore, the use of pg/ml was standardized when indicating pro-inflammatory cytokine levels according to the instructions provided with the ELISA kits. Therefore, the units of pro-inflammatory cytokines were different from those of digestive enzyme activity.

PM count in ascites. After centrifuging the mouse peritoneal fluid, the supernatant was poured into an Eppendorf tube and retained. Subsequently, 1 ml PBS was added to the pellet and mixed, after which, 20 μl of the suspension was added to an automated cell counter (Countstar; Shanghai Ruiyu Biotechnology Co., Ltd.), and the total number of PMs was counted.

Histological examination of pancreatic tissue. The pancreatic tissue was fixed in 4% paraformaldehyde at 4˚C for 24 h, embedded in paraffin and cut into 3- to 4-μm sections. The sections were stained with in hematoxylin solution for 10 min, with color separation in acid water and ammonia for 3 sec each, rinsed in running water for 1 h and then put into distilled water. Sections were dehydrated in 70 and 90% alcohol for 10 min each, and then stained with eosin staining solution for 3 min at room temperature using an ST5010 AutoStainer (Leica Microsystems GmbH). Finally, the changes in pulmonary histopathology were observed under a BX43 light microscope (Olympus Corporation).

Immunohistochemistry. Pancreatic sections were deparaffinized using xylene and hydrated in different concentrations of ethanol, 100, 95, 90, 85 and 70% for 5 min each, and then rinsed in tap water for 10 min, before being treated with citrate antigen repair solution (pH 6.0) at 100˚C for 18 min. The sections were then treated with 3% H_2O_2 at 37˚C for 10 min to block endogenous peroxidase, blocked with goat serum (from cat. no. E-IR-R-217 kit) for 30 min at 37˚C, and then incubated with anti-TLR4 (1:50), anti-LC3 (1:100) and anti-Beclin-1 (1:50) antibodies at 4˚C for 18 h. Subsequently, the sections were incubated with polyperoxidase-anti-mouse/rabbit IgG (from cat. no. E-IR-R-217 kit) at 37˚C for 30 min, with DAB for 30 sec and with hematoxylin at room temperature for 10 min. After 10 sec of differentiation solution fractionation configured from 5% ethanol hydrochloride, the sections were dehydrated through a concentration gradient of ethanol and xylene, sealed with neutral resin and images were captured under a light microscope. Semi-quantification of protein expression was performed in three randomly selected regions using ImageJ software version 1.54d (National Institutes of Health). The average optical density value is obtained by dividing the cumulative optical density by the area of the effective target distribution. Dark brown staining of cells indicated a positive signal.

Transmission electron microscopy. The pancreatic tissues were fixed in 2.5% glutaraldehyde fixative at 4˚C for 24 h, dehydrated through a graded ethanol series and embedded in epoxy resin for pre-polymerization at 45˚C for 12 h, then polymerized at 60˚C for 24 h. After staining with toluidine blue, the pancreatic tissues were sectioned to a thickness of 1-3 μm using an ultrathin sectioning machine. The obtained sections were double stained with uranyl acetate and lead nitrate for 30 min at room temperature, and were then observed using transmission electron microscopy (JEM-1400Plus; Japan Electronics Co., Ltd.).

Treatment of macrophages with AS. Mouse PMs were isolated, grown and adhered to 96-well plates ($5.0x10^4$ cells/well) at 37˚C in 5% CO_2 for 4 h. AS (20 μg/ml) in serum-free DMEM was added after attachment, and after 2 h of incubation at 37˚C in 5% CO_2, the cells in the 96-well plates were stimulated with TP (1, 5 and 20 μg/ml) or LPS (1, 3 and 9 ng/ml). After 4 h of incubation at 37˚C in 5% CO_2, the supernatants were collected to detect TNF-α and IL-6 levels.

RAW264.7 cells were grown to confluence in 96-well plates ($5.0x10^4$ cells/well), washed twice and incubated with serum-free DMEM for 12 h. AS (35 μg/ml) in serum-free DMEM was added after attachment, and after 2 h of incubation at 37˚C in 5% CO_2, the cells in the 96-well plates were stimulation with TP (10 μg/ml) or different concentrations of LPS (1, 3 and 9 μg/ml). After 4 h of incubation, the supernatants were collected to detect TNF-α levels (TP10 + LPS9 only made two independent samples, while the other groups had three independent samples).

Treatment of macrophages with autophagy inhibitor. Mouse PMs ($5.0x10^4$ cells/well) were grown on 96-well plates at 37˚C in 5% CO_2 for 4 h. LY294002 (10 μM) or LY294002 (10 μM) combined with AS (20 μg/ml) in serum-free DMEM was added after attachment, and after 2 h of incubation at 37˚C in 5% CO_2, the cells were stimulated with TP (5 μg/ml) or LPS (1 ng/ml) for 4 h at 37˚C in 5% CO_2. Subsequently, the supernatants were collected to detect TNF-α and IL-6 levels.

AS treatment of AR42J cells. AR42J cells ($5.0x10^4$ cells/well) were grown to confluence in 96-well plates, washed twice and incubated with F12K culture medium (containing 10% FBS) for 24 h at 37˚C in 5% CO_2. After CR (0.5 nM) or LPS (0.1, 0.3 and 0.9 μg/ml) were added (only three independent samples for the Medium, LPS0.1 and LPS0.3 groups, while the other groups had four independent samples), the cells were treated with AS (0.5 μg/ml) for 24 h at 37˚C in 5% CO_2 (only three independent samples for the Medium group, while the other groups had four independent samples). Thereafter, the supernatants were collected to detect amylase activity.

Immunofluorescence staining. RAW264.7 cells ($1.0x10^5$ cells/well) in 24-well plates (each well plus coverslips) were treated with AS (35 μg/ml) for 2 h at 37˚C in 5% CO_2, and then treated with TP (10 μg/ml) and/or LPS (3 ng/ml) for 1 h at 37˚C in 5% CO_2. The cells were collected and fixed in 4% paraformaldehyde for 1 h at room temperature, after which, blocking was performed with goat serum for 1 h at room temperature. After incubating the slides with polyclonal antibodies against LC3 (1:100) at 4˚C for 24 h, the slides were washed with PBS, and then incubated with fluorescein isothiocyanate-labeled goat anti-rabbit IgG antibody (1:200; from cat. no. P0179 kit) for 24 h at 4˚C. Finally, the slides were washed with PBS and the cell nuclei were stained with 1 mg/ml DAPI for 5 min at room temperature. After PBS washing and glycerol mounting, the LC3 levels in the cells were observed using fluorescence microscopy (BX43; Olympus Corporation).

HBAD-mRFP-GFP-LC3 infection analysis. RAW264.7 cells ($1.0x10^4$/well) in 24-well plates (each well plus coverslips) were infected with autophagic double-labeled adenovirus mRFP-GFP-LC3 at $1x10^8$ PFU/ml for 8 h at 37˚C in 5% CO_2 according to the manufacturer's instructions, and then the virus-containing medium was aspirated and the cells were washed twice with PBS. Subsequently, RAW264.7 cells in 24-well plates were treated with AS (35 μg/ml) for 2 h at 37˚C in 5% CO_2, and then treated with TP (10 μg/ml) and/or LPS (3 ng/ml) for 1 h at 37˚C in 5% CO_2. After the cells were collected, PBS was added and the cells were washed twice, and then 400 μl paraformaldehyde was added and fixed for 20 min at room temperature. A small amount of fluorescence quencher was added to the slide in advance. After fixation with paraformaldehyde, the slides were washed with PBS, and the plates were observed under a laser confocal microscope and images were captured (STELLARIS5; Leica Microsystems GmbH).

Assays of pro-inflammatory cytokine levels and enzyme activities. The TNF-α and IL-6 levels in the mouse serum, pancreatic homogenates, lavage fluid and cellular supernatant were measured using ELISA kits according to the manufacturer's protocols. The activities of amylase in the mouse serum and cellular supernatant, and TP and SOD in the pancreatic homogenates, were determined using their respective enzyme activity assay kits.

WB. Total protein was extracted from RAW264.7 cells and mouse pancreatic tissues using the Total Protein Extraction Kit, and the protein concentration was determined by BCA Protein Concentration Measurement Kit (Enhanced) (cat. no. P0009; Beyotime Institute of Biotechnology). Equal amounts (20 μg) of proteins were supersampled. LC3 was separated by 15% sodium dodecyl sulfate polyacrylamide gel electrophoresis, and the rest of the proteins were separated by 10% sodium dodecyl sulfate polyacrylamide gel electrophoresis, followed by transfer to polyvinylidene fluoride membranes and blocked with 5% skimmed milk for 2 h at room temperature. After cutting the membranes according to different molecular weights, anti-LC3 (1:1,000), anti-ATG16L1 (1:1,000), anti-TLR4 (1:1,000), anti-MyD88 (1:1,000), anti-TRAF6 (1:1,000), anti-Bcelin-1 (1:1,000), anti-β-actin (1:1,000) and anti-GAPDH (1:1,000) antibodies were incubated at 4˚C for 18 h. Subsequently, the chemiluminescent substrates were enhanced with HRP-conjugated goat anti-rabbit secondary antibody (1:2,000) or anti-mouse secondary antibody (1:2,000) for 1 h at room temperature. Subsequently, the membrane regeneration solution (cat. no. SW3020; Beijing Solarbio Science & Technology Co., Ltd.) was used to elute the antibodies and the membranes were incubated again with alternative primary antibodies, followed by further incubation with horseradish peroxidase-conjugated secondary antibodies. Chemiluminescent-labeled immunoreactive protein bands were visualized using the ChemiDoc™ Touch imaging system and the SuperSignal chemiluminescent substrate (both from Bio-Rad Laboratories, Inc.), and were analyzed using the ImageJ software package.

Statistical analysis. Data are presented as the mean ± SD and each experiment was performed in triplicate. Data from each group were statistically analyzed using one-way ANOVA and Tukey's post hoc test using GraphPad Prism 8.4.2 software (Dotmatics). $P<0.05$ was considered to indicate a statistically significant difference.

Results

AS significantly alleviates damage to the pancreatic tissue in AP model mice. To investigate the therapeutic effect of AS on a mouse model of AP induced by CR combined with LPS, the general condition of the pancreatic tissue, the pancreatic coefficient and pathological changes in the pancreatic tissue were observed.

Gross observation showed that the surface of the pancreatic tissue in the NS group was smooth, with no bleeding spots; however, the pancreatic tissue from the mice in the AP group was swollen, gray-colored, and there were a number of saponified and bleeding points on the tissue surface (Fig. 1A). AS treatment (5 and 15 mg/kg) did not reduce the edema of the pancreatic tissues but reduced the number of bleeding points, and adhesion between pancreatic tissues and surrounding tissues could be observed to be markedly reduced during the sampling process. Furthermore, the pancreatic coefficient was high in the AP group compared with NS group but was decreased in the AS treatment groups (Fig. 1B).

Histopathological observation of pancreatic tissue showed that in the NS group, the pancreatic lobular septum was clear, the acinar arrangement was regular and no obvious changes were observed (Fig. 1C). In the AP group, the pancreatic tissue structure was disorganized, the septa of the lobules were markedly enlarged, large coagulated necrosis was observed in the glandular parenchyma, which was accompanied by bleeding, and a large number of inflammatory cells infiltrated around the necrotic lesion. In the AP + AS5 and AP + AS15 groups, pancreatic hemorrhage, necrosis and inflammatory cell infiltration were reduced compared with those in the AP group. The effect in the AP + AS15 group was more obvious than that in the AP + AS5 group. These results indicated that AS reduced the degree of pancreatic tissue damage in a mouse model of AP.

AS reduces both the activation of enzymes and the levels of pro-inflammatory cytokines in pancreatic tissue. Enzyme activation is a hallmark of AP (23); in particular, TP activity is closely related to the severity of pancreatitis. The activation of pancreatic enzymes and the levels of pro-inflammatory cytokines in pancreatic tissue are closely related to the degree of local inflammatory response in the pancreatic tissue, as well as the subsequent systemic inflammatory response (24).

The results of the present study showed that pancreatic TP activity was significantly increased in the AP group compared with that in the NS group, whereas AS (5 and 15 mg/ml) significantly decreased its activity (Fig. 2A). Furthermore, compared with those in the NS group, pancreatic TNF-α and IL-6 levels were significantly increased in the AP group, but were significantly decreased in the AP + AS15 group (Fig. 2B and C).

Excessive production of oxygen free radicals is closely related to the inflammatory state of the human body, and SOD serves an important role in scavenging oxygen free radicals (25,26). Therefore, SOD activity was assessed in pancreatic tissue. The results showed that the SOD activity was significantly decreased in the AP group compared with that in the NS group, but was significantly increased in the AS groups (Fig. 2D).

AS reduces pancreatic enzyme activity and pro-inflammatory cytokine levels in the blood. Pancreatic enzymes that are released in response to pancreatic tissue damage enter the bloodstream; therefore, the serum levels of pancreatic enzymes are closely related to the severity of pancreatitis (27). In particular, the activity of pancreatic amylase in the blood is closely related to the severity of pancreatitis (27). In the present study, pancreatic amylase activity was investigated. The results showed that the activity of serum amylase was significantly increased in the AP group compared with that in the NS group, but was significantly decreased in the AP + AS group (Fig. 3A).

The local inflammatory response in pancreatitis can trigger a systemic inflammatory response known as SIRS; therefore, pro-inflammatory cytokine levels are strongly associated with local and systemic inflammation during AP (28,29). In the present study, the serum levels of TNF-α and IL-6 were investigated. The results showed the levels of TNF-α and IL-6 in the AP group were significantly increased compared with those in the NS group, but were significantly decreased in the AS groups (Fig. 3B and C).

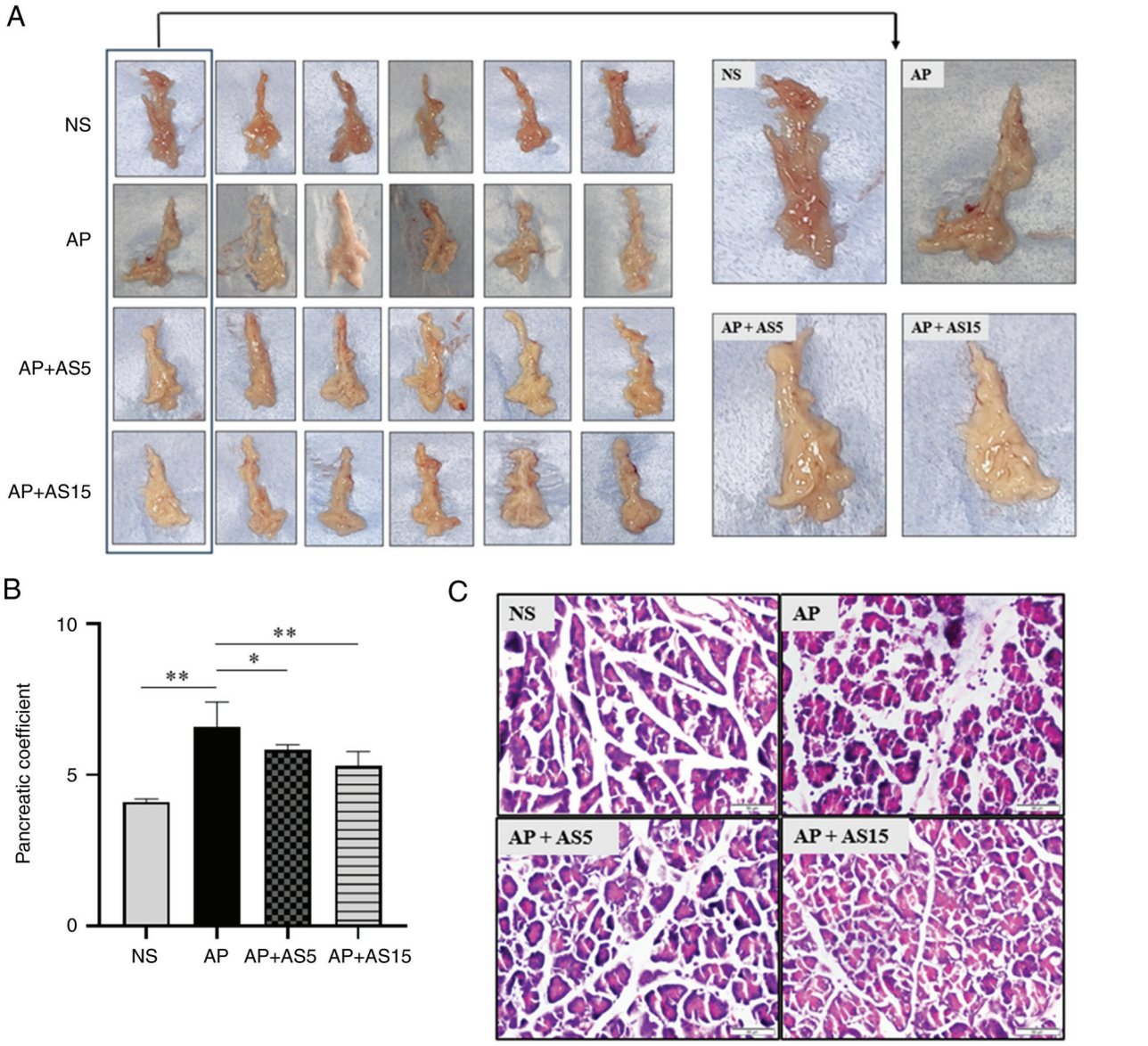

Figure 1. AS significantly alleviates the damage to pancreatic tissues in a mouse model of AP. (A) Gross observation of pancreatic tissues at the 2 h time point (n=6). (B) Pancreatic coefficient at the 8 h time point (n=6). (C) Hematoxylin and eosin staining of the pancreatic tissues at the 2 h time point. Magnification, x40. Data are presented as the mean ± SD and were analyzed by one-way ANOVA and Tukey's test. *P<0.05, **P<0.01. AP, acute pancreatitis; AS, artesunate; NS, normal saline.

AS significantly reduces the levels of pro-inflammatory cytokines and the number of PMs in the peritoneal lavage fluid. Macrophages are a major source of pro-inflammatory cytokine production. The peritoneal cavity contains a large number of macrophages, and the number and function of PMs are closely related to the severity of pancreatitis (30,31).

The results of the present study showed that compared with that in the NS group, the total number of PMs in the AP group was significantly increased; however, AS treatment significantly decreased the total number of PMs (Fig. 4A). The levels of TNF-α and IL-6 in the peritoneal lavage fluid were significantly higher in the AP group than those in the NS group, whereas AS significantly decreased TNF-α levels (Fig. 4B and C).

AS inhibits autophagy and TLR4 signaling pathway-related proteins in vivo. Autophagy serves an important role in the pathophysiological process of AP. In the late stage of autophagy, autophagic lysosomes with a single membrane are present (32). Transmission electron microscopy showed no autophagic abnormalities in the NS group, whereas a large number of autophagic lysosomes were apparent in the AP group compared with that in the NS group; however, almost no autophagic lysosomes were observed in the AP + AS15 group (Fig. 5A).

LC3 is a molecular hallmark for the occurrence of autophagy in cells (33) and autophagy-related gene (ATG) is also involved in regulating the formation of cellular autophagosomes (34). The present study observed the changes in LC3 and ATG16L1 in the pancreatic tissues of mice with AP. Immunohistochemistry results showed that LC3 protein expression was significantly increased in the AP group compared with that in the NS group, whereas it was significantly decreased in the AS groups (Fig. 5B). WB results showed that LC3II and ATG16L1 protein expression

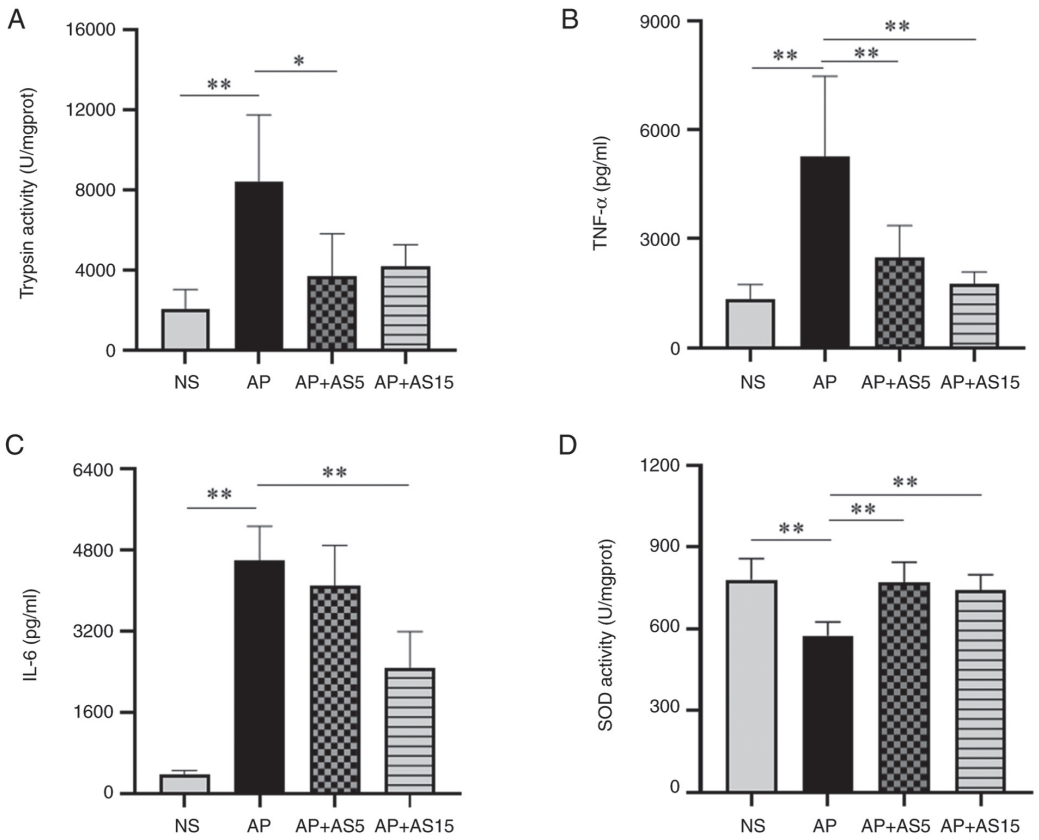

Figure 2. AS significantly reduces pancreatic enzyme activity and the levels of pro-inflammatory cytokines in pancreatic tissues. (A) Trypsin activity 18 h after AP establishment (n=4-5). (B) TNF-α levels, (C) IL-6 levels and (D) SOD activity in pancreatic tissues at the 2 h time point (n=6). Data are presented as the mean ± SD and were analyzed by one-way ANOVA and Tukey's test. *P<0.05, **P<0.01. AP, acute pancreatitis; AS, artesunate; IL, interleukin; NS, normal saline; SOD, superoxide dismutase; TNF-α, tumor necrosis factor α.

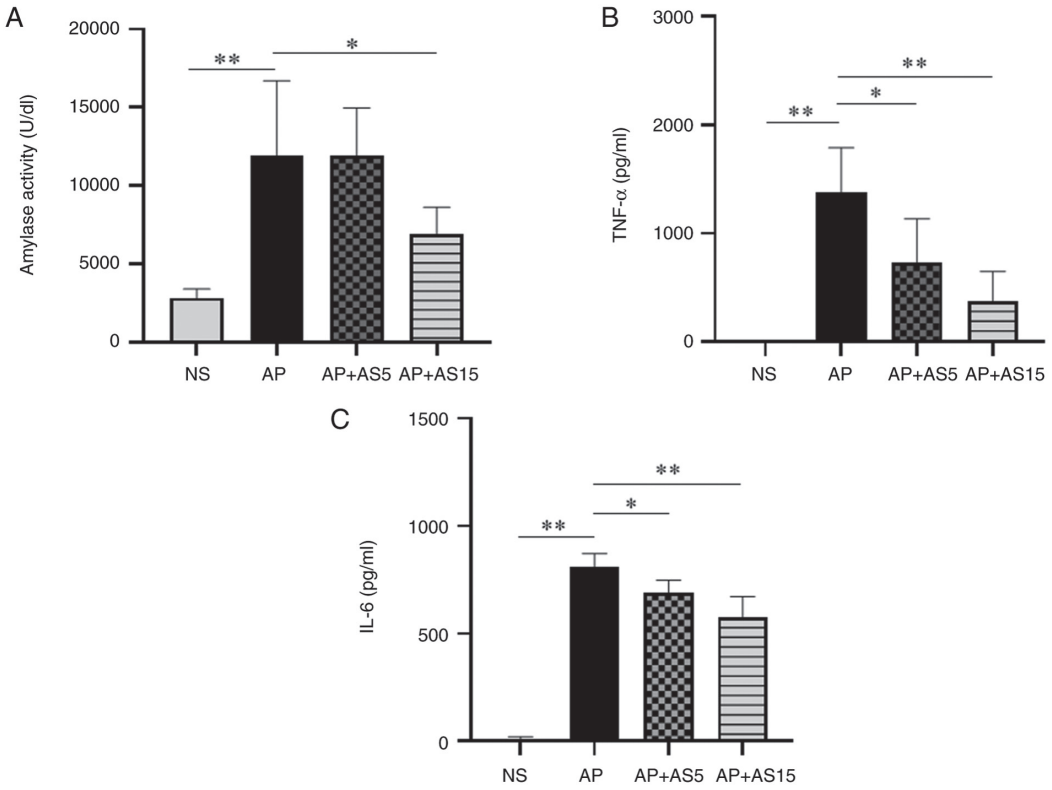

Figure 3. AS significantly reduces pancreatic enzyme activity and the levels of pro-inflammatory cytokines in the blood. (A) Amylase activity, (B) TNF-α levels and (C) IL-6 levels in the serum at the 2 h time point (n=6). Data are presented as the mean ± SD and were analyzed by one-way ANOVA and Tukey's test. *P<0.05, **P<0.01. AP, acute pancreatitis; AS, artesunate; IL, interleukin; NS, normal saline; TNF-α, tumor necrosis factor α.

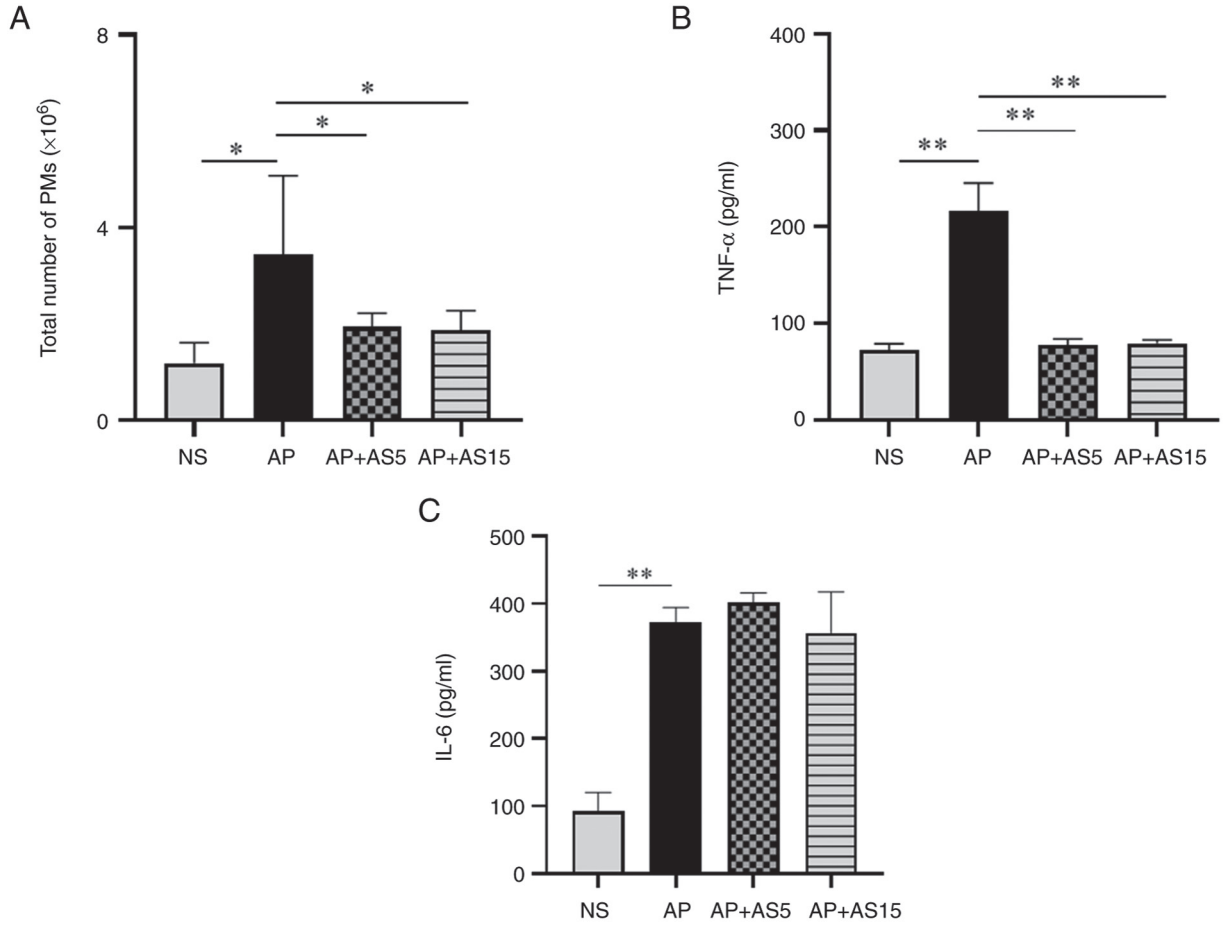

Figure 4. AS significantly reduces the levels of pro-inflammatory cytokines and the number of PMs in the peritoneal lavage fluid of AP mice. (A) Total number of PMs, (B) TNF-α levels and (C) IL-6 levels in the peritoneal lavage fluid at the 2 h time point (n=6). Data are presented as the mean ± SD and were analyzed by one-way ANOVA and Tukey's test. *P<0.05, **P<0.01. AP, acute pancreatitis; AS, artesunate; IL, interleukin; NS, normal saline; PM, peritoneal macrophage; TNF-α, tumor necrosis factor α.

levels were significantly increased in the AP group compared with those in the NS group, whereas they were significantly decreased in the AS groups (Fig. 5C). These results indicated that AS may inhibit the expression of key molecules in the autophagy pathway in the pancreatic tissues of mice with AP.

The LPS-induced autophagy process is closely related to the TLR4/TRAF6/Beclin-1 signaling pathway (35); therefore, immunohistochemistry and WB were used to detect changes in the expression levels of important molecules in the TLR4 signaling pathway in the pancreatic tissues of mice with AP, and further observed the effects of AS on inflammation and autophagy. Immunohistochemistry showed that the protein expression levels of TLR4 and Beclin-1 were significantly increased in the AP group compared with those in the NS group, whereas they were significantly decreased in the AS groups (Fig. 5D and E). The results of WB showed that the expression levels of MyD88, TRAF6 and Beclin-1 were significantly increased in the AP group compared with those in the NS group, whereas they were significantly decreased in the AS groups (Fig. 5F). These findings indicated that AS inhibited the expression of molecules related to the TLR4/TRAF6/Beclin-1 signaling pathway in the pancreatic tissues of mice with AP.

AS inhibits the release of pro-inflammatory cytokines from mouse macrophages treated with TP and LPS in vitro. Macrophages serve important roles in the occurrence and development of AP (36,37), and TP and LPS can induce macrophages to release pro-inflammatory cytokines (19,38); however, whether TP combined with LPS could synergistically induce the release of more pro-inflammatory cytokines than TP or LPS alone is unclear. In the present study, both the mouse RAW264.7 cell line and PMs were used to determine the effect of TP combined with LPS.

Firstly, PMs were treated with a low concentration of LPS (1 ng/ml) combined with different concentrations of TP (1, 5 and 20 μg/ml). After 4 h, the cell supernatant was collected and the levels of TNF-α in the supernatant were detected. The results showed that LPS and different concentrations of TP could induce TNF-α release; however, TP5 + LPS1 group could induce significantly higher TNF-α release (Fig. 6A). In addition, PMs were treated with TP (5 μg/ml) combined with different concentrations of LPS (1, 3 and 9 ng/ml). The results also showed that the TP5 + LPS1 group could induce significantly more TNF-α release (Fig. 6B). The TNF-α levels induced by the combination of LPS (1 ng/ml) and TP (5 μg/ml) were significantly higher than those using either factor alone; therefore, 1 ng/ml LPS plus 5 μg/ml TP were used in subsequent experiments in PMs.

Secondly, the effects of TP plus LPS on TNF-α were validated in RAW264.7 cells. RAW264.7 cells were treated

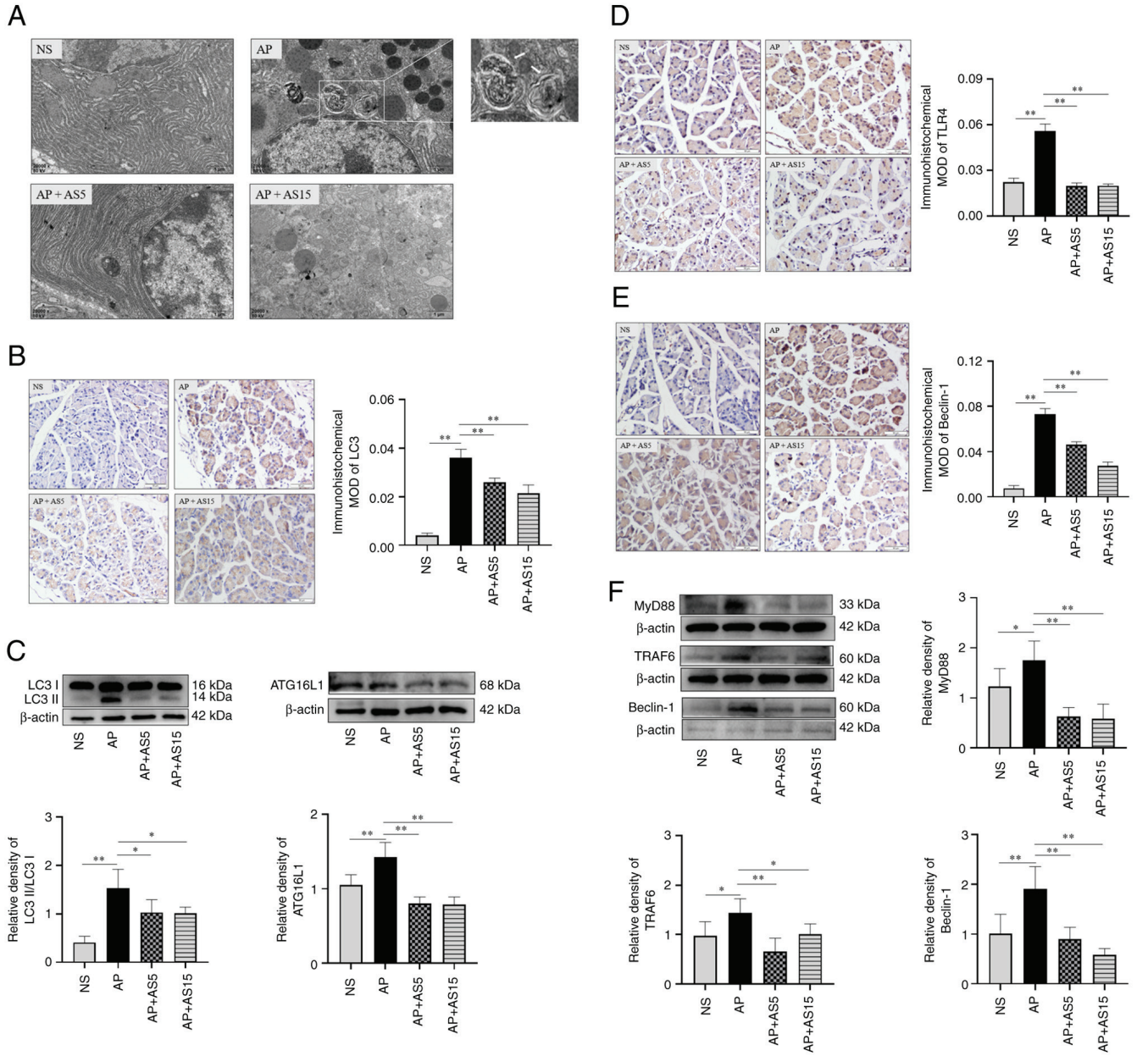

Figure 5. AS inhibits autophagy and TLR4 signaling pathway-related protein expression in AP model mice. (A) Representative transmission electron microscopy images of pancreatic tissues at the 2 h time point. White arrows indicate autophagic lysosomes. Magnification, x20,000. (B) Immunohistochemical analysis of LC3 protein expression in pancreatic tissues at the 2 h time point (n=3). A dark brown color in the cells indicates a positive signal. (C) Western blot analysis of LC3II and ATG16L1 protein expression in the pancreatic tissues of mice with AP at the 2 h time point (n=6). Immunohistochemical analysis of (D) TLR4 and (E) Beclin-1 protein expression in pancreatic tissues at the 2 h time point (n=3). A dark brown color in the cells indicates a positive signal. Magnification, x40. (F) Western blotting of MyD88, TRAF6 and Beclin-1 protein expression in the pancreatic tissues of mice with AP at the 2 h time point (n=6). Data are presented as the mean ± SD and were analyzed by one-way ANOVA and Tukey's test. *P<0.05, **P<0.01. AP, acute pancreatitis; AS, artesunate; ATG, autophagy-related gene; LC3, microtubule associated protein 1 light chain 3; MOD, mean optical density; MyD88, myeloid differentiation primary response 88; NS, normal saline; TLR4, Toll-like receptor 4; TRAF6, tumor necrosis factor receptor associated factor 6.

with TP (10 μg/ml) combined with different concentrations of LPS (1, 3 and 9 ng/ml) for 4 h. The RAW264.7 cell validation results were consistent with those detected using PMs (Fig. 6C). Based on the aforementioned results, a combination of 10 μg/ml TP with 3 ng/ml LPS was selected for subsequent experiments using RAW264.7 cells.

Furthermore, the effects of AS (20 and 35 μg/ml) on PMs and RAW264.7 cells treated with TP and LPS were observed. The results showed that AS significantly inhibited the release of TNF-α and IL-6 induced by TP combined with LPS in PMs (Fig. 6D and E). The results in RAW264.7 cells were consistent with those in PMs (Fig. 6F and G). These results demonstrated that TP combined with LPS could significantly increase the release of pro-inflammatory cytokines from mouse macrophages, whereas AS could markedly inhibit this pro-inflammatory cytokine release.

AS decreases the amylase activity induced by CR combined with LPS in vitro. Parenchymal cells release large amounts of pancreatic enzymes, but less pro-inflammatory cytokines, to participate in inflammation (39). Cholecystokinin can induce pancreatic acinar cells to produce amylase (40). CR is a gastric

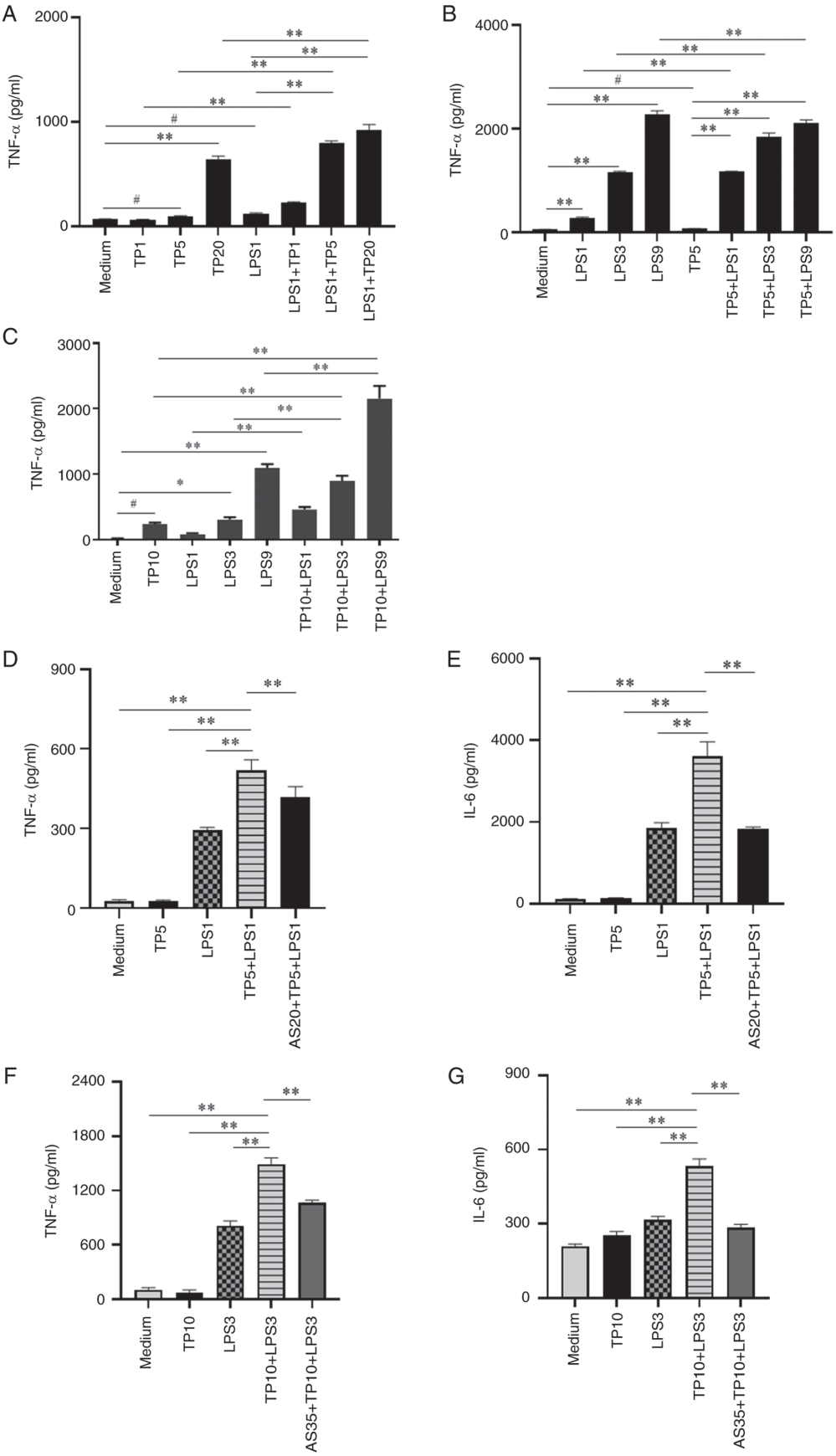

Figure 6. TP combined with LPS increases the release of pro-inflammatory cytokines from mouse macrophages, whereas AS inhibits their release. (A) LPS combined with different concentrations of TP induced the release of TNF-α by PMs (n=3). (B) TP combined with different concentrations of LPS induced the release of TNF-α by PMs (n=3). (C) TNF-α levels in the supernatant of TP and LPS-treated RAW264.7 cells (n=2-3). Effect of AS on the release of (D) TNF-α and (E) IL-6 from PMs treated with LPS combined with TP (n=3). Effect of AS on the release of (F) TNF-α and (G) IL-6 from RAW264.7 cells treated with LPS combined with TP (n=3). Data are presented as the mean ± SD and were analyzed by one-way ANOVA and Tukey's test. *P<0.05, **P<0.01; $^{\#}$P>0.05. AS, artesunate; IL, interleukin; LPS, lipopolysaccharide; PM, peritoneal macrophage; TNF-α, tumor necrosis factor α; TP, trypsin.

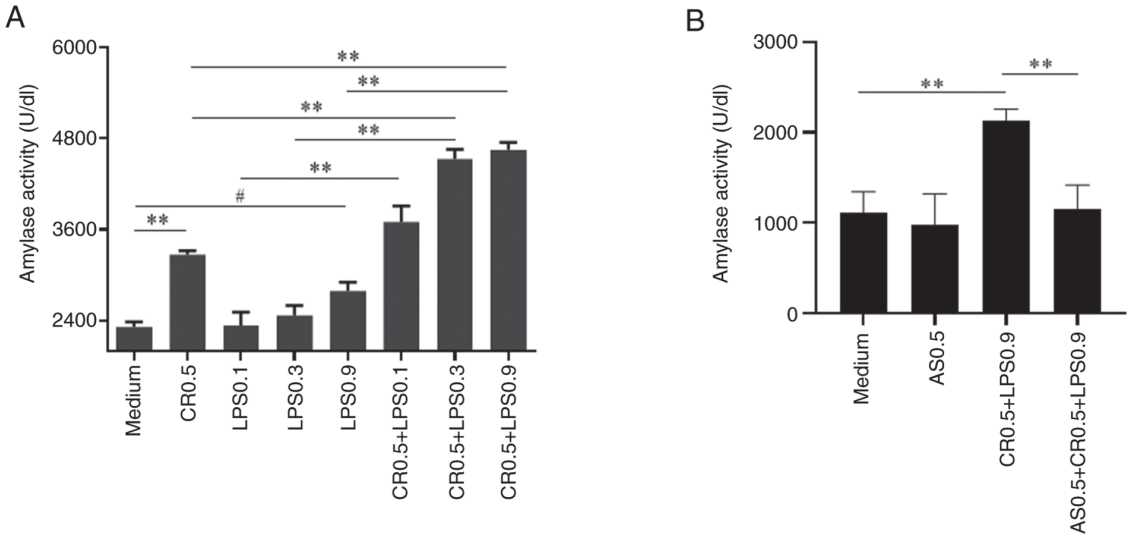

Figure 7. CR combined with LPS increases the activity of amylase in acinar cells, whereas AS decreases the activity of amylase. (A) Activity of amylase in the supernatant of AR42J cells treated with CR combined with LPS (n=3-4). (B) AS reduced the amylase activity in the supernatant of AR42J cells treated with CR in combination with LPS (n=3-4). Data are presented as the mean ± SD and were analyzed by one-way ANOVA and Tukey's test. **P<0.01; $^{\#}$P>0.05. AS, artesunate; CR, cerulein; LPS, lipopolysaccharide.

regulatory molecule similar to cholecystokinin in function and composition, which can stimulate the secretion of amylase from the stomach, bile duct and pancreas; therefore, CR is often used in animal and cell experiments to replace cholecystokinin (41-43). In the present study, CR combined with LPS was used to treat the AR42J acinar cell line, and the amylase activity in acinar cells was measured.

The results showed that either 0.5 nM CR or 0.9 μg/ml LPS alone could significantly increase amylase activity compared with that in the control (Medium) group, whereas 0.9 μg/ml LPS combined with 0.5 nM CR significantly increased the amylase activity compared with that induced by either factor alone (Fig. 7A). Thus, the combination of 0.5 nM CR and 0.9 μg/ml LPS was selected for subsequent experiments. Based on the aforementioned experiments, the effect of AS (0.5 μg/ml) on amylase activity was investigated. The results showed that AS significantly decreased the amylase activity induced by CR combined with LPS (Fig. 7B).

Autophagy serves an important role in the release of pro-inflammatory cytokines, and AS inhibits autophagy and TLR4 signaling pathway-related proteins in vitro. To detect whether macrophages treated with TP combined with LPS induced excessive autophagy in AP, the effects of the autophagy inhibitor LY294002 (10 μM) on the release of TNF-α and IL-6 induced by LPS (1 ng/ml) and TP (5 μg/ml) were observed in PMs. The results showed that LY294002 could significantly decrease the levels of TNF-α and IL-6 released by PMs treated with TP combined with LPS (Fig. 8A and B), Subsequently, the effects of AS (20 μg/ml) combined with the autophagy inhibitor LY294002 (10 μM) were observed on the release of TNF-α and IL-6 induced by LPS (1 ng/ml) and TP (5 μg/ml) in PMs. The results showed that both AS and LY294002 could significantly decrease the levels of TNF-α and IL-6 released by PMs treated with TP combined with LPS (Fig. 8C and D). However, compared with in the group treated with AS or LY294002 alone, the combination of AS and LY294002 did not further reduce the levels of TNF-α and IL-6 induced by LPS and TP.

To observe the effects of AS on autophagy, the HBDA-mRFP-GFP-LC3 adenovirus was used to monitor autophagic flow in real-time; mRFP can be used to label and track LC3, and the attenuation of GFP indicates the fusion of lysosomes and autophagosomes to form autolysosomes. The results showed that the number of autophagosomes and autolysosomes was significantly increased after TP (10 μg/ml) combined with LPS (3 ng/ml) treatment in RAW264.7 cells; however, AS (35 μg/ml) significantly reduced the number of autophagosomes and autolysosomes (Fig. 8E-H), suggesting that AS could inhibit the excessive autophagy stimulated by TP combined with LPS in RAW264.7 cells.

Secondly, WB results showed that the protein expression levels of LC3II were significantly increased after TP (10 μg/ml) combined with LPS (3 ng/ml) treatment in RAW264.7 cells compared with that in the control (Medium) group, whereas AS (35 μg/ml) significantly decreased the protein expression levels of LC3II (Fig. 8I).

Furthermore, immunofluorescence microscopy showed that TP (10 μg/ml) and LPS (3 ng/ml), alone or in combination, increased the expression of LC3 compared with that in the control group, whereas AS (35 μg/ml) notably decreased the expression of LC3 in RAW264.7 cells (Fig. 8J). These results demonstrated that the effect of AS on the release of pro-inflammatory cytokines may be closely related to the inhibition of autophagy. Subsequently, the present study observed whether TP (10 μg/ml) combined with LPS (3 ng/ml) induced changes in important molecules (TLR4, Myd88, TRAF6 and Beclin-1) in the TLR4 signaling pathway in RAW264.7 cells. The results showed that TP combined with LPS increased the protein expression levels of TLR4, Myd88, TRAF6 and Beclin-1 in RAW264.7 cells compared with those in the control (Medium) group, whereas AS (35 μg/ml) significantly decreased their protein expression levels (Fig. 8K).

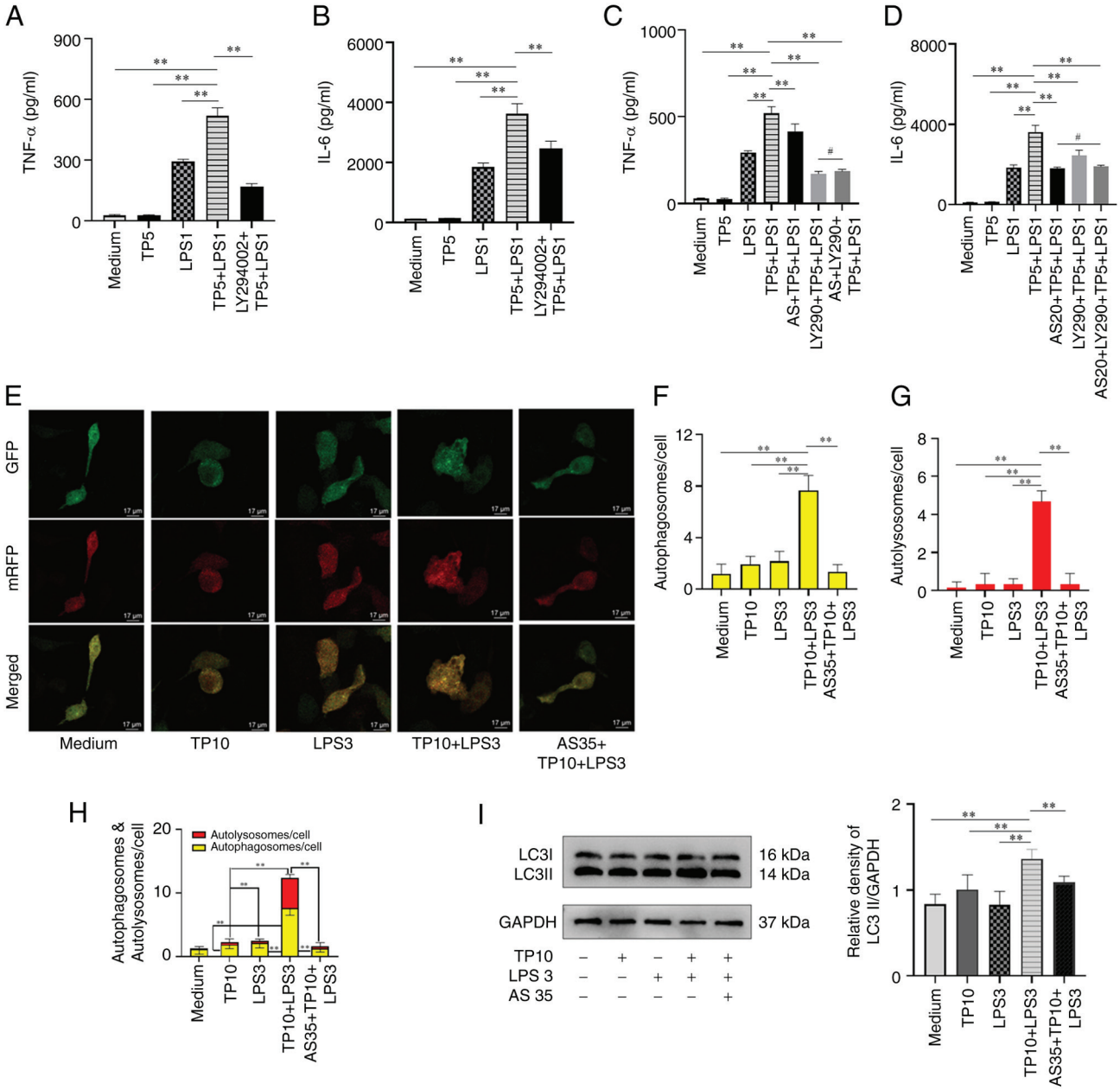

Figure 8. Continued.

Discussion

The results of the present study suggested that AS has a protective effect on AP in mice induced by LPS combined with CR, in which it reduces pro-inflammatory cytokine release and pancreatic enzyme levels, and attenuates pancreatic tissue damage. Furthermore, it was indicated that the molecular mechanism of AS treatment of AP may be closely related to inhibition of the TLR4/NF-κB signaling pathway and autophagic signaling.

Most AP models have been performed in rodents, and the commonly used methods are pancreatic duct ligation (44), intraperitoneal injection of an L-arginine inducer (45), retrograde injection of sodium taurocholate into the biliopancreatic duct (46), and intraperitoneal injection of CR into the pancreatic duct (47). Our previous study established a rat model of AP using retrograde injection of sodium taurocholate into the biliopancreatic duct, which produced AP that was similar in severity to the human disease (16). However, it is not an ideal model of AP-MODS because it requires surgery and delicate manipulation, and is not easily replicated (48). Therefore, an AP model that has the advantages of being noninvasive, easy to perform and reproducible was chosen for the present study, namely intraperitoneal injection of LPS combined with CR, which also increases the severity of AP and MODS compared with the AP model established using CR alone (49,50), and mimics AP-related sepsis (51).

The present results showed that the mouse pancreatic tissues developed lesions characterized by interstitial edema, hemorrhage and necrotic acinar cells in response to LPS combined with CR. In addition, enhanced amylase and TP activities, significantly elevated levels of pro-inflammatory

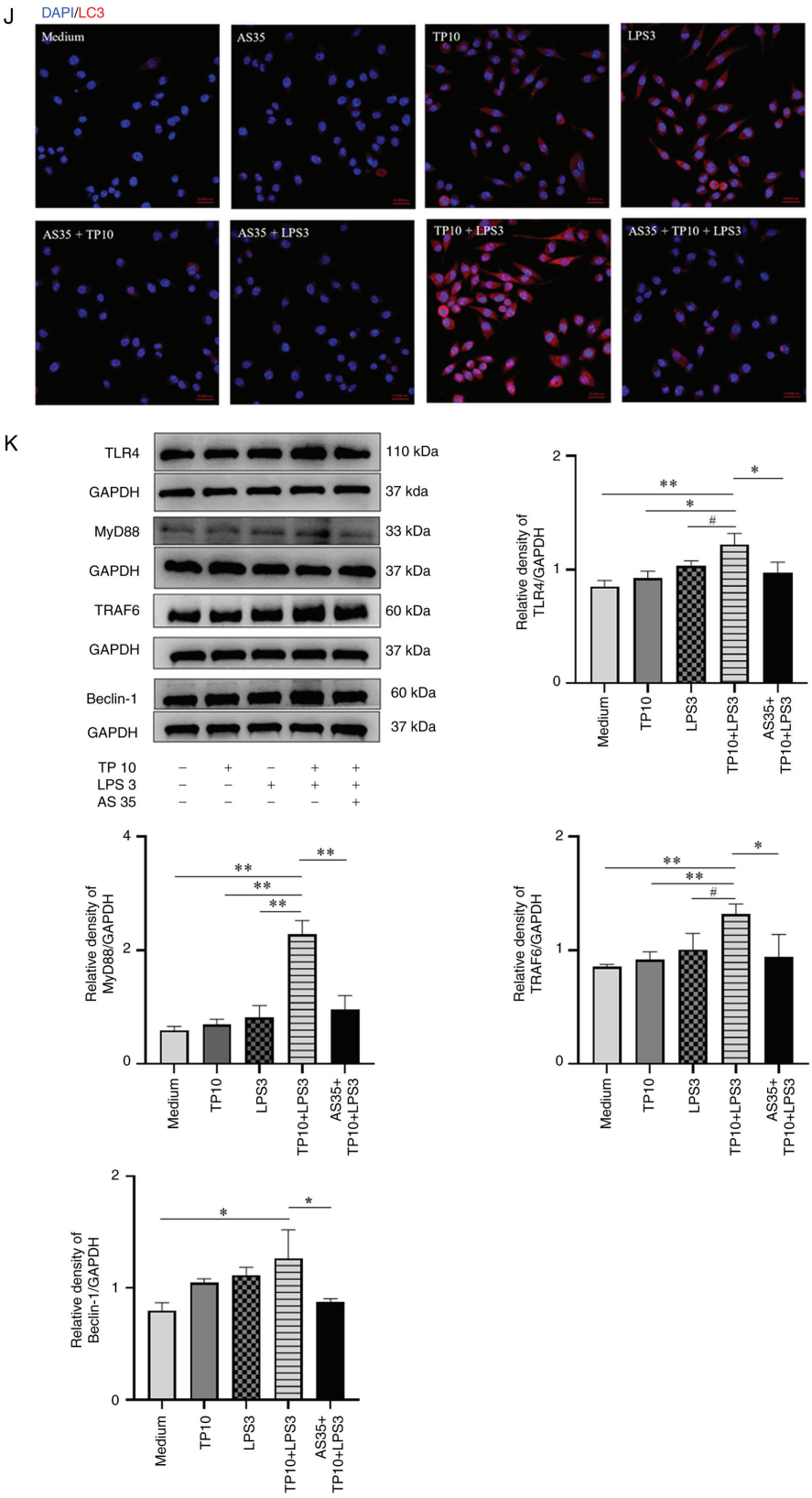

Figure 8. AS inhibits the protein expression levels of key molecules associated with TLR4-dependent autophagy in PMs and RAW264.7 cells. Autophagy inhibitor LY294002 significantly inhibited (A) TNF-α and (B) IL-6 release from PMs induced by TP combined with LPS (n=3). AS combined with autophagy inhibitor LY294002 had no significant effect on the release of (C) TNF-α and (D) IL-6 from PMs induced by TP combined with LPS (n=3). (E) AS inhibited autophagic flow induced by TP combined with LPS in RAW264.7 cells (n=3). Autophagosomes (yellow) and autolysosomes (red) were observed and counted. Scale bar, 17 μm. Number of (F) autophagosomes, (G) autolysosomes, and (H) autophagosomes and autolysosomes. AS inhibited LC3II protein expression induced by TP combined with LPS in RAW264.7 cells, as determined by (I) western blotting and (J) laser scanning confocal microscope. Magnification, x400. (K) AS inhibited the protein expression levels of TLR4, MyD88, TRAF6 and Beclin-1 in RAW264.7 cells treated with TP combined with LPS (n=3). Data are presented as the mean ± SD and were analyzed by one-way ANOVA and Tukey's test. *P<0.05, **P<0.01; $^{\#}$P>0.05. AS, artesunate; GFP, green fluorescent protein; IL, interleukin; LC3, microtubule associated protein 1 light chain 3; LPS, lipopolysaccharide; mRFP, monomeric red fluorescent protein; MyD88, myeloid differentiation primary response 88; NS, normal saline; TLR4, Toll-like receptor 4; TNF-α, tumor necrosis factor α; TRAF6, TNF receptor associated factor 6; TP, trypsin.

cytokines and PM counts, and significantly decreased SOD activity suggested that LPS combined with CR could be used to successfully establish a mouse model of AP.

AP is an acute gastrointestinal disorder with high morbidity and mortality rates (52,53). The severe systemic inflammation induced by AP frequently leads to the development of MODS and subsequent death (54,55). The pathogenesis of AP is complex, and although numerous studies have been conducted to gain a better understanding of its pathophysiology (56,57), and several clinical drug trials have been performed, including those applying protease inhibitors, such as ulinastatin and somatostatin (58), their therapeutic efficacy remains questionable (59). There is no effective treatment for AP; therefore, the search for effective and safe drugs has become an important research goal in the treatment of AP.

AS, a sesquiterpene lactone obtained from the plant *Artemisia annua* (60), is a stable derivative of artemisinin and is an effective drug used to treat malaria, improve inflammation and treat tumors (such as lung and liver cancer) (61,62). Our previous study showed that AS can inhibit the TLR4/NF-κB signaling pathway to reduce digestive enzyme activity and pro-inflammatory cytokine expression, thereby improving the survival rate of rats with SAP (16). Therefore, the role of AS was investigated in the present mouse model of AP, and the results suggested that AS may produce significant inflammatory protection in mice with AP.

In the diagnosis of AP, digestive enzymes are highly sensitive and specific markers (63). In addition, oxygen radicals are involved in the process of pancreatic necrosis (25). Therefore, the activities of amylase, TP and SOD in mice can reflect the severity of AP in the model and the therapeutic effect of drugs. In addition to digestive enzymes, pro-inflammatory cytokines released by local macrophages, alveolar cells and distal macrophages are markers of AP severity (64). The mononuclear macrophage system serves an important role in maintaining internal environment stability. PMs are mononuclear macrophages, the number and functional status of which can reflect the state of the macrophage system; therefore, the total number of PMs is important in AP (65).

In the present study, the results indicated that although the edema of pancreatic tissues in mice with AP was not reduced after the administration of AS, the adhesion between pancreatic tissues and surrounding tissues could be observed to be markedly reduced during the sampling process, and the number of hemorrhagic spots was reduced. Moreover, AS could reduce the pancreatic coefficient, pancreatic hemorrhage, necrosis and inflammatory cell infiltration in mice; all of these results indicated that AS could reduce the degree of pancreatic injury in mice with AP. Moreover, AS not only significantly decreased serum amylase and TP activities, and increased SOD activity, in mice with AP, but also significantly decreased TNF-α and IL-6 levels in the serum, pancreatic tissue and peritoneal lavage fluid. In addition, the number of PMs was significantly reduced after AS treatment. This suggested that PMs are important in AP and that AS could reduce the inflammatory response in mice with AP by reducing the levels of pro-inflammatory cytokines and digestive enzymes, and increasing the activity of SOD.

During the development of SAP, LPS induces the release of large amounts of pro-inflammatory cytokines from macrophages and acinar cells, which are involved in the pathophysiological process of pancreatitis development and promote the progression from local to systemic inflammation (13,66). AR42J cells treated with a combination of CR and LPS exhibited markers of more severe pancreatitis, including enhanced secretion of digestive enzymes and pro-inflammatory cytokines, compared with CR stimulation alone, as well as less apoptosis and substantial evidence of necrosis (67), which is more conducive to the therapeutic effect of drugs in AP. Therefore, the present study established a cellular model of AP by treating AR42J cells with CR combined with LPS, which was consistent with models generated in national and international studies, and previous results from our laboratory (68,69). The present results showed that CR combined with LPS could induce a further increase in the level of secreted amylase activity in AR42J cells compared with CR and LPS alone, with a significant synergistic effect. These findings suggested that CR combined with LPS could successfully establish a cell model of AP.

Both TP and NF-κB activation, which are independent events (70), can be observed in the early stages of AP, and can further exacerbate pancreatic tissue damage and the systemic inflammatory response. Activated TP and intestinal-transported LPS coexist during AP; therefore, LPS can amplify the TP-induced inflammatory response, and the same TP can also amplify the LPS-induced inflammatory response, which could better mimic the pathological process of AP. Therefore, the present study established a cellular model of AP by treating macrophages with LPS combined with TP. The results showed that small doses of LPS combined with TP could induce a large release of TNF-α and IL-6 from PMs, with a significant synergistic effect, which was more effective than that induced by LPS or TP alone. The synergistic effect was also verified in RAW264.7 cells. This result suggested that LPS combined with TP could successfully establish a cell model of AP.

The levels of pro-inflammatory cytokines and digestive enzyme activity in the supernatants of the three cell models were observed, the results showed that AS significantly reduced the levels of TNF-α and IL-6, and amylase activity, suggesting that AS could exert its anti-inflammatory effects by inhibiting digestive enzyme activity and the release of pro-inflammatory cytokines.

It has been reported that activation of trypsinogen may be associated with abnormal autophagy in pancreatic cells. Moreover, excessive autophagy could be involved in, or induced by, the development of an excessive inflammatory response (71,72). During AP, autophagy is activated, but is impaired and incomplete. It has been shown that aberrant autophagy in pancreatic cells caused by excessive activation of autophagy or blockade of the autophagic pathway promotes the development and progression of AP (73). Therefore, the present study determined the effects of the autophagy inhibitor LY294002 on TP combined with LPS-stimulated PMs, and showed that it could inhibit the release of pro-inflammatory cytokines from PMs. This suggested that autophagy may be aberrantly activated during AP and that AP is closely related to autophagy. However, after treatment with a combination of AS and the autophagy inhibitor, the levels of TNF-α and IL-6 were not further reduced, thus it was hypothesized that the effects

of AS and autophagy inhibitors may be the same, and both inhibit excessive autophagy.

TLR4 is an important component of the innate immune response that has an important role in the recognition of and defense against invading pathogens. LPS activates TLR4 in a MyD88-dependent manner, triggering a classical inflammatory cascade response, leading to the activation of NF-κB and the release of pro-inflammatory cytokines (74). The TLR4/NF-κB signaling pathway and autophagic pathways serve important roles not only in immune cells, but also in AR42J acinar cells (75-77). The current gold standard for the detection of autophagy is the observation of autophagosomes by electron microscopy and the detection of the autophagy marker LC3 (78). During autophagy, LC3I is modified and processed to produce LC3II, which is localized to autophagic vesicles. Thus, both LC3 and LC3II present in autophagic vesicles are used as molecular markers for the occurrence of autophagy in cells, and the amount of LC3II is proportional to the degree of autophagy (79). Beclin-1 is also a key molecular marker of autophagy (80). The present results showed that AS not only decreased LC3 and ATG16L1 protein levels, and reduced autophagic lysosome production, but also significantly inhibited the protein expression levels of TLR4, MyD88, TRAF6 and Beclin-1 in the LPS combined with CR-induced mouse model of AP, suggesting that the therapeutic effects of AS on the AP model mice are closely related to the TLR4/NF-κB signaling pathway and autophagy. In the LPS combined with TP-induced RAW264.7 cell inflammation model, AS was observed to reduce the number of autophagosomes and autolysosomes under laser confocal microscopy; and AS reduced the protein expression levels of LC3II, TLR4, MyD88, TRAF6 and Beclin-1. The immunofluorescence results also showed that AS significantly reduced the excessive elevation of LC3 induced by TP combined with LPS stimulation in RAW264.7 cells. In combination, these results suggested that the mechanism by which AS exerts its anti-inflammatory effects on AP might be closely related to inhibition of TLR4/NF-κB and autophagic signaling pathways.

In conclusion, AS exhibited a significant protective effect toward mice with AP via a mechanism that could be related to inhibition of the TLR4/NF-κB and autophagy signaling pathways, and reduction in digestive enzyme activity and pro-inflammatory cytokine expression. Therefore, AS may be considered as a valuable therapeutic agent for AP.

Acknowledgements

Not applicable.

Funding

This work was supported by grants from the National Natural Science Foundation of China (grant no. 81673495), the Major National Science and Technology Program of China for Innovative Drug (grant no. 2017ZX09101002-002-009), the National Natural Science Foundation of China-Guizhou Provincial People's Government Joint Fund Project (grant no. NSFC-U1812403-4-1) and the Fourth Batch of 'Thousand People Innovation and Entrepreneurship Talents Fund' in Guizhou Province.

Availability of data and materials

The data generated in the present study may be requested from the corresponding author.

Authors' contributions

DL, CL, FD and HZ substantially contributed to the experimental conception and design of the study. FO and RQ contributed to the acquisition of data and analysis of *in vitro* experiments. DL, CL, FD, ZZ, YW, YZ and ML contributed to the animal experiments. HZ, XL, XP, YH and YC contributed to statistical analysis and visualization. DL, XL and HZ are responsible for manuscript writing. HZ supervised all experiments. DL, CL and FD confirm the authenticity of all the raw data. All authors have read and approved the final version of the manuscript. All authors took responsibility for the integrity and accuracy of the study.

Ethics approval and consent to participate

Ethics approval for the animal experiments was obtained from the Ethical Committee of Zunyi Medical University [approval no. ZMU (2020) 2-296]. All animal experiments conducted in the present study followed the guidelines and regulations specified in this ethical approval.

Patient consent for publication

Not applicable.

Competing interests

The authors declare that they have no competing interests.

References

1. Greenberg JA, Hsu J, Bawazeer M, Marshall J, Friedrich JO, Nathens A, Coburn N, May GR, Pearsall E and McLeod RS: Clinical practice guideline: Management of acute pancreatitis. Can J Surg 59: 128-140, 2016.
2. Tenner S, Baillie J, Dewitt J and Vege SS; American College of Gastroenterology: American college of gastroenterology guideline: Management of acute pancreatitis. Am J Gastroenterol 108: 1400-1416, 2013.
3. Meher S, Mishra TS, Sasmal PK, Rath S, Sharma R, Rout B and Sahu MK: Role of biomarkers in diagnosis and prognostic evaluation of acute pancreatitis. J Biomark 2015: 519534, 2015.
4. Habtezion A, Gukovskaya AS and Pandol SJ: Acute pancreatitis: A multifaceted set of organelle and cellular interactions. Gastroenterology 156: 1941-1950, 2019.
5. Ge P, Luo Y, Okoye CS, Chen H, Liu J, Zhang G, Xu C and Chen H: Intestinal barrier damage, systemic inflammatory response syndrome, and acute lung injury: A troublesome trio for acute pancreatitis. Biomed Pharmacother 32: 110770, 2020.
6. Yuan X, Wu J, Guo X, Li W, Luo C, Li S, Wang B, Tang L and Sun H: Autophagy in acute pancreatitis: Organelle interaction and microRNA regulation. Oxid Med Cell Longev 2021: 8811935, 2021.
7. Banks PA, Bollen TL, Dervenis C, Gooszen HG, Johnson CD, Sarr MG, Tsiotos GG and Vege SS; Acute Pancreatitis Classification Working Group: Classification of acute pancreatitis-2012: Revision of the Atlanta classification and definitions by international consensus. Gut 62: 102-111, 2013.
8. Vege SS, Dimagno MJ, Forsmark CE, Martel M and Barkun AN: Initial medical treatment of acute pancreatitis: American gastroenterological association institute technical review. Gastroenterology 154: 1103-1139, 2018.

9. Dumnicka P, Maduzia D, Ceranowicz P, Olszanecki R, Drożdż R and Kuśnierz-Cabala B: The interplay between inflammation, coagulation and endothelial injury in the early phase of acute pancreatitis: Clinical implications. Int J Mol Sci 18: 354, 2017.
10. Kuo CEA, Wu SY, Lee CH, Lai YR, Lu CH, Chen PC, Cheng JH, Tsai LY, Yen KT, Tsao Y and Tsai SM: Toona sinensis modulates autophagy and cytokines in lipopolysaccharide-induced RAW 264.7 macrophages. Biomed Pharmacother 129: 110386, 2020.
11. Dawra R, Sah RP, Dudeja V, Rishi L, Talukdar R, Garg P and Saluja AK: Intra-acinar trypsinogen activation mediates early stages of pancreatic injury but not inflammation in mice with acute pancreatitis. Gastroenterology 141: 2210-2217.e2, 2011.
12. Liu J, Huang L, Luo M and Xia X: Bacterial translocation in acute pancreatitis. Crit Rev Microbiol 45: 539-547, 2019.
13. Li J, Wu Y, Zhang S, Zhang J, Ji F, Bo W, Guo X and Li Z: Baicalein protect pancreatic injury in rats with severe acute pancreatitis by inhibiting pro-inflammatory cytokines expression. Biochem Biophys Res Commun 466: 664-669, 2015.
14. Roussel C, Caumes E, Thellier M, Ndour PA, Buffet PA and Jauréguiberry S: Artesunate to treat severe malaria in travellers: Review of efficacy and safety and practical implications. J Travel Med 24: taw093, 2017.
15. Lei XY, Tan RZ, Jia J, Wu SL, Wen CL, Lin X, Wang H, Shi ZJ, Li B, Kang Y and Wang L: Artesunate relieves acute kidney injury through inhibiting macrophagic Mincle-mediated necroptosis and inflammation to tubular epithelial cell. J Cell Mol Med 25: 8775-8788, 2021.
16. Cen Y, Liu C, Li X, Yan Z, Kuang M, Su Y, Pan X, Qin R, Liu X, Zheng J and Zhou H: Artesunate ameliorates severe acute pancreatitis (SAP) in rats by inhibiting expression of pro-inflammatory cytokines and Toll-like receptor 4. Int Immunopharmacol 38: 252-260, 2016.
17. National Research Council (US): Committee for the Update of the Guide for the Care and Use of Laboratory Animals: Guide for the care and use of laboratory animals. 8th edition. National Academies Press, Washington, DC, 2011.
18. Zhang W, Wang G, Xu ZG, Tu H, Hu F, Dai J, Chang Y, Chen Y, Lu Y, Zeng H, *et al*: Lactate is a natural suppressor of RLR signaling by targeting MAVS. Cell 178: 176-189.e15, 2019.
19. Luo J, Wang N, Hua L, Deng F, Liu D, Zhou J, Yuan Y, Ouyang F, Chen X, Long S, *et al*: The anti-sepsis effect of isocorydine screened from guizhou ethnic medicine is closely related to upregulation of vitamin d receptor expression and inhibition of NFκB p65 translocation into the nucleus. J Inflamm Res 15: 5649-5664, 2022.
20. Li X, He C, Li N, Ding L, Chen H, Wan J, Yang X, Xia L, He W, Xiong H, *et al*: The interplay between the gut microbiota and NLRP3 activation affects the severity of acute pancreatitis in mice. Gut Microbes 11: 1774-1789, 2020.
21. Zhang W, Xie Z, Fang X, Wang Z, Li Z, Shi Y, Wang X, Li L and Wang X: Laboratory animal ethics education improves medical students' awareness of laboratory animal ethics. BMC Med Educ 24: 709, 2024.
22. Nomenclature Committee of the International Union of Biochemistry (NC-IUB): 'Units of Enzyme Activity'. Eur J Biochem 97: 319-320, 1979.
23. Geokas MC, Baltaxe HA, Banks PA, Silva J Jr and Frey CF: Acute pancreatitis. Ann Intern Med 103: 86-100, 1985.
24. Wang GJ, Gao CF, Wei D, Wang C and Ding SQ: Acute pancreatitis: Etiology and common pathogenesis. World J Gastroenterol 15: 1427-1430, 2009.
25. Armstrong JA, Cash N, Soares PMG, Souza MHLP, Sutton R and Criddle DN: Oxidative stress in acute pancreatitis: Lost in translation? Free Radic Res 47: 917-933, 2013.
26. Fernández-Sánchez A, Madrigal-Santillán E, Bautista M, Esquivel-Soto J, Morales-González A, Esquivel-Chirino C, Durante-Montiel I, Sánchez-Rivera G, Valadez-Vega C and Morales-González JA: Inflammation, oxidative stress, and obesity. Int J Mol Sci 12: 3117-3132, 2011.
27. Sheehan SJ, Lee JH, Wells CK and Topazian M: Serum amylase, pancreatic stents, and pancreatitis after sphincter of Oddi manometry. Gastrointest Endosc 62: 260-265, 2005.
28. Jang DI, Lee AH, Shin HY, Song HR, Park JH, Kang TB, Lee SR and Yang SH: The role of tumor necrosis factor alpha (TNF-α) in autoimmune disease and current TNF-α Inhibitors in therapeutics. Int J Mol Sci 22: 2719, 2021.
29. Shapouri-Moghaddam A, Mohammadian S, Vazini H, Taghadosi M, Esmaeili SA, Mardani F, Seifi B, Mohammadi A, Afshari JT and Sahebkar A: Macrophage plasticity, polarization, and function in health and disease. J Cell Physiol 233: 6425-6440, 2018.
30. Dijkstra CD, Döpp EA, Joling P and Kraal G: The heterogeneity of mononuclear phagocytes in lymphoid organs: Distinct macrophage subpopulations in rat recognized by monoclonal antibodies ED1, ED2 and ED3. Adv Exp Med Biol 186: 409-419, 1985.
31. Mikami Y, Takeda K, Shibuya K, Qiu-Feng H, Shimamura H, Yamauchi J, Egawa S, Sunamura M, Yagi H, Endo Y and Matsuno S: Do peritoneal macrophages play an essential role in the progression of acute pancreatitis in rats? Pancreas 27: 253-260, 2003.
32. Gros F and Muller S: The role of lysosomes in metabolic and autoimmune diseases. Nat Rev Nephrol 19: 366-383. 2023.
33. Mareninova OA, Jia W, Gretler SR, Holthaus CL, Thomas DDH, Pimienta M, Dillon DL, Gukovskaya AS, Gukovsky I and Groblewski GE: Transgenic expression of GFP-LC3 perturbs autophagy in exocrine pancreas and acute pancreatitis responses in mice. Autophagy 16: 2084-2097, 2020.
34. Li X, He S and Ma B: Autophagy and autophagy-related proteins in cancer. Mol Cancer 19: 12, 2020.
35. Ngowi EE, Sarfraz M, Afzal A, Khan NH, Khattak S, Zhang X, Li T, Duan SF, Ji XY and Wu DD: Roles of hydrogen sulfide donors in common kidney diseases. Front Pharmacol 11: 564281, 2020.
36. Hu F, Lou N, Jiao J, Guo F, Xiang H and Shang D: Macrophages in pancreatitis: Mechanisms and therapeutic potential. Biomed Pharmacother 131: 110693, 2020.
37. Sendler M, Weiss FU, Golchert J, Homuth G, Van Den Brandt C, Mahajan UM, Partecke LI, Döring P, Gukovsky I, Gukovskaya A, *et al*: Cathepsin B-mediated activation of trypsinogen in endocytosing macrophages increases severity of pancreatitis in mice. Gastroenterology 154: 704-718.e10, 2018.
38. Saluja A, Dudeja V, Dawra R and Sah RP: Early intra-acinar events in pathogenesis of pancreatitis. Gastroenterology 156: 1979-1993, 2019.
39. Yasunaga K, Ito T, Miki M, Ueda K, Fujiyama T, Tachibana Y, Fujimori N, Kawabe K and Ogawa Y: Using CRISPR/Cas9 to knock out amylase in acinar cells decreases pancreatitis-induced autophagy. Biomed Res Int 2018: 8719397, 2018.
40. Selig L, Sack U, Gaiser S, Klöppel G, Savkovic V, Mössner J, Keim V and Bödeker H: Characterisation of a transgenic mouse expressing R122H human cationic trypsinogen. BMC Gastroenterol 6: 30, 2006.
41. Singh VK, Wu BU, Bollen TL, Repas K, Maurer R, Mortele KJ and Banks PA: Early systemic inflammatory response syndrome is associated with severe acute pancreatitis. Clin Gastroenterol Hepatol 7: 1247-1251, 2009.
42. Lankisch PG, Assmus C, Lehnick D, Maisonneuve P and Lowenfels AB: Acute pancreatitis: Does gender matter? Dig Dis Sci 46: 2470-2474, 2001.
43. Mukherjee R, Mareninova OA, Odinokova IV, Huang W, Murphy J, Chvanov M, Javed MA, Wen L, Booth DM, Cane MC, *et al*: Mechanism of mitochondrial permeability transition pore induction and damage in the pancreas: Inhibition prevents acute pancreatitis by protecting production of ATP. Gut 65: 1333-1346, 2016.
44. Zhang L, Wu Z, Tong Z, Yao Q, Wang Z and Li W: Vagus nerve stimulation decreases pancreatitis severity in mice. Front Immunol 11: 595957, 2021.
45. Qi-Xiang M, Yang F, Ze-Hua H, Nuo-Ming Y, Rui-Long W, Bin-Qiang X, Jun-Jie F, Chun-Lan H and Yue Z: Intestinal TLR4 deletion exacerbates acute pancreatitis through gut microbiota dysbiosis and Paneth cells deficiency. Gut Microbes 14: 2112882, 2022.
46. Li H, Xie J, Guo X, Yang G, Cai B, Liu J, Yue M, Tang Y, Wang G, Chen S, *et al*: Bifidobacterium spp. and their metabolite lactate protect against acute pancreatitis via inhibition of pancreatic and systemic inflammatory responses. Gut Microbes 14: 2127456, 2022.
47. Baron TH, DiMaio CJ, Wang AY and Morgan KA: American gastroenterological association clinical practice update: Management of pancreatic necrosis. Gastroenterology 158: 67-75.e1, 2020.
48. Sah RP, Garg P and Saluja AK: Pathogenic mechanisms of acute pancreatitis. Curr Opin Gastroenterol 28: 507-515, 2012.
49. Biczo G, Vegh ET, Shalbueva N, Mareninova OA, Elperin J, Lotshaw E, Gretler S, Lugea A, Malla SR, Dawson D, *et al*: Mitochondrial dysfunction, through impaired autophagy, leads to endoplasmic reticulum stress, deregulated lipid metabolism, and pancreatitis in animal models. Gastroenterology 154: 689-703, 2018.
50. Wu JS, Li WM, Chen YN, Zhao Q and Chen QF: Endoplasmic reticulum stress is activated in acute pancreatitis. J Dig Dis 17: 295-303, 2016.

51. Lu G, Tong Z, Ding Y, Liu J, Pan Y, Gao L, Tu J, Wang Y, Liu G and Li W: Aspirin protects against acinar cells necrosis in severe acute pancreatitis in mice. Biomed Res Int 2016: 6089430, 2016.
52. Sendler M, Dummer A, Weiss FU, Krüger B, Wartmann T, Scharffetter-Kochanek K, Van Rooijen N, Malla SR, Aghdassi A, Halangk W, *et al*: Tumour necrosis factor α secretion induces protease activation and acinar cell necrosis in acute experimental pancreatitis in mice. Gut 62: 430-439, 2013.
53. Munir F, Jamshed MB, Shahid N, Hussain HM, Muhammad SA, Mamun AA and Zhang Q: Advances in immunomodulatory therapy for severe acute pancreatitis. Immunol Lett 217: 72-76, 2020.
54. Mayer J, Rau B, Gansauge F and Beger HG: Inflammatory mediators in human acute pancreatitis: Clinical and pathophysiological implications. Gut 47: 546-552, 2000.
55. Mentula P, Kylänpää ML, Kemppainen E, Jansson SE, Sarna S, Puolakkainen P, Haapiainen R and Repo H: Early prediction of organ failure by combined markers in patients with acute pancreatitis. Br J Surg 92: 68-75, 2005.
56. Noh KW, Pungpapong S, Wallace MB, Woodward TA and Raimondo M: Do cytokine concentrations in pancreatic juice predict the presence of pancreatic diseases? Clin Gastroenterol Hepatol 4: 782-789, 2006.
57. Shimizu K: Pancreatic stellate cells: Molecular mechanism of pancreatic fibrosis. J Gastroenterol Hepatol 23 (Suppl 1): S119-S121, 2008.
58. Horváth IL, Bunduc S, Fehérvári P, Váncsa S, Nagy R, Garmaa G, Kleiner D, Hegyi P, Erőss B and Csupor D: The combination of ulinastatin and somatostatin reduces complication rates in acute pancreatitis: A systematic review and meta-analysis of randomized controlled trials. Sci Rep 12: 17979, 2022.
59. Cohen J, Vincent JL, Adhikari NKJ, Machado FR, Angus DC, Calandra T, Jaton K, Giulieri S, Delaloye J, Opal S, *et al*: Sepsis: A roadmap for future research. Lancet Infect Dis 15: 581-614, 2015.
60. Bhattacharjee S, Coppens I, Mbengue A, Suresh N, Ghorbal M, Slouka Z, Safeukui I, Tang HY, Speicher DW, Stahelin RV, *et al*: Remodeling of the malaria parasite and host human red cell by vesicle amplification that induces artemisinin resistance. Blood 131: 1234-1247, 2018.
61. Zhao D, Zhang J, Xu G and Wang Q: Artesunate protects LPS-induced acute lung injury by inhibiting TLR4 expre-ssion and inducing Nrf2 activation. Inflammation 40: 798-805, 2017.
62. Gugliandolo E, D'amico R, Cordaro M, Fusco R, Siracusa R, Crupi R, Impellizzeri D, Cuzzocrea S and Di Paola R: Neuroprotective effect of artesunate in experimental model of traumatic brain injury. Front Neurol 9: 590, 2018.
63. Yang RW, Shao ZX, Chen YY, Yin Z and Wang WJ: Lipase and pancreatic amylase activities in diagnosis of acute pancreatitis in patients with hyperamylasemia. Hepatobiliary Pancreat Dis Int 4: 600-603, 2005.
64. Schneider L, Jabrailova B, Strobel O, Hackert T and Werner J: Inflammatory profiling of early experimental necrotizing pancreatitis. Life Sci 126: 76-80, 2015.
65. Zhou X, Li W, Wang S, Zhang P, Wang Q, Xiao J, Zhang C, Zheng X, Xu X, Xue S, *et al*: YAP aggravates inflammatory bowel disease by regulating M1/M2 macrophage polarization and gut microbial homeostasis. Cell Rep 27: 1176-1189.e5, 2019.
66. Zhang X, Kang Y, Li X, Huang Y, Qi R, Han Y, Cai R, Gao Y and Qi Y: Potentilla discolor ameliorates LPS-induced inflammatory responses through suppressing NF-κB and AP-1 pathways. Biomed Pharmacother 144: 112345, 2021.
67. Liu Y, Yang L, Chen KL, Zhou B, Yan H, Zhou ZG and Li Y: Knockdown of GRP78 promotes apoptosis in pancreatic acinar cells and attenuates the severity of cerulein and LPS induced pancreatic inflammation. PLoS One 9: e92389, 2014.
68. Liu Y, Zhou ZG, Chen KL, Zhou B, Yang L, Yan H and Li Y: The ER chaperone GRP78 is associated with the severity of cerulein-induced pancreatic inflammation via regulating apoptosis of pancreatic acinar cells. Hepatogastroenterology 59: 1670-1676, 2012.
69. Wu L, Cai B, Liu X and Cai H: Emodin attenuates calcium overload and endoplasmic reticulum stress in AR42J rat pancreatic acinar cells. Mol Med Rep 9: 267-272, 2014.
70. Mayerle J, Sendler M, Hegyi E, Beyer G, Lerch MM and Sahin-Tóth M: Genetics, cell biology, and pathophysiology of pancreatitis. Gastroenterology 156: 1951-1968.e1, 2019.
71. Banks PA and Freeman ML; Practice Parameters Committee of the American College of Gastroenterology: Practice guidelines in acute pancreatitis. Am J Gastroenterol 101: 2379-2400, 2006.
72. Gloor B, Müller CA, Worni M, Martignoni ME, Uhl W and Büchler MW: Late mortality in patients with severe acute pancreatitis. Br J Surg 88: 975-979, 2001.
73. Wang X, Zhou G, Liu C, Wei R, Zhu S, Xu Y, Wu M and Miao Q: Acanthopanax versus 3-methyladenine ameliorates sodium taurocholate-induced severe acute pancreatitis by inhibiting the autophagic pathway in rats. Mediators Inflamm 2016: 8369704, 2016.
74. Hoque R, Farooq A, Ghani A, Gorelick F and Mehal WZ: Lactate reduces liver and pancreatic injury in Toll-like receptor- and inflammasome-mediated inflammation via GPR81-mediated suppression of innate immunity. Gastroenterology 146: 1763-1774, 2014.
75. Wang Y, Wang G, Cui L, Liu R, Xiao H and Yin C: Angiotensin 1-7 ameliorates caerulein-induced inflammation in pancreatic acinar cells by downregulating Toll-like receptor 4/nuclear factor-κB expression. Mol Med Rep 17: 3511-3518, 2018.
76. Chang RJ, Wang HL, Qin MB, Liang ZH, He JP, Wei YL, Fu HZ and Tang GD: Ghrelin inhibits IKKβ/NF-κB activation and reduces pro-inflammatory cytokine production in pancreatic acinar AR42J cells treated with cerulein. Hepatobiliary Pancreat Dis Int 20: 366-375, 2021.
77. Sun H, Tian J and Li J: MiR-92b-3p ameliorates inflammation and autophagy by targeting TRAF3 and suppressing MKK3-p38 pathway in caerulein-induced AR42J cells. Int Immunopharmacol 88: 106691, 2020.
78. Wang S, Ni HM, Chao X, Wang H, Bridges B, Kumer S, Schmitt T, Mareninova O, Gukovskaya A, De Lisle RC, *et al*: Impaired TFEB-mediated lysosomal biogenesis promotes the development of pancreatitis in mice and is associated with human pancreatitis. Autophagy 15: 1954-1969, 2019.
79. Han F, Xiao QQ, Peng S, Che XY, Jiang LS, Shao Q and He B: Atorvastatin ameliorates LPS-induced inflammatory response by autophagy via AKT/mTOR signaling pathway. J Cell Biochem 119: 1604-1615, 2018.
80. Cicchini M, Karantza V and Xia B: Molecular pathways: Autophagy in cancer-a matter of timing and context. Clin Cancer Res 21: 498-504, 2015.